energies

MDPI

Article

Optimal Planning of Multitype DGs and D-STATCOMs in Power Distribution Network Using an Efficient Parameter Free Metaheuristic Algorithm

Subrat Kumar Dash [1], Sivkumar Mishra [2,*], Almoataz Youssef Abdelaziz [3], Junhee Hong [4] and Zong Woo Geem [4,*]

[1] Department of Electrical Engineering, Goverrnment College of Engineering Kalahandi, Bhawanipatna 766002, Odisha, India; dashsubratkumar@gmail.com
[2] Department of Electrical Engineering, Center for Advanced Post Graduate Studies, Biju Patnaik University of Technology, Rourkela 769015, Odisha, India
[3] Faculty of Engineering and Technology, Future University in Egypt, Cairo 11835, Egypt; ayabdelaziz63@gmail.com
[4] Department of Smart City & Energy, Gachon University, Seongnam 13120, Korea; hongpa@gachon.ac.kr
* Correspondence: sivmishra@gmail.com (S.M.); geem@gachon.ac.kr (Z.W.G.)

Abstract: In a quest to solve the multi-objective optimal planning problem using a simple parameter-free metaheuristic algorithm, this paper establishes the recently proposed student psychology-based optimization (SPBO) algorithm as the most promising one, comparing it with the other two popular nonparametric metaheuristic optimization algorithms, i.e., the symbiotic organisms search (SOS) and Harris hawk optimization (HHO). A novel multi-objective framework (with suitable weights) is proposed with a real power loss minimization index, bus voltage variation minimization index, system voltage stability maximization index, and system annual cost minimization index to cover various technical, economic, and environmental aspects. The performances of these three algorithms are compared extensively for simultaneous allocation of multitype distributed generations (DGs) and D-STACOM in 33-bus and 118-bus test systems considering eight different cases. The detailed analysis also includes the statistical analysis of the results obtained using the three algorithms applied to the two test distribution systems.

Keywords: distributed generators; simultaneous allocation; D-STATCOM; student psychology-based optimization; Harris hawk optimization; symbiotic organism search optimization

Citation: Dash, S.K.; Mishra, S.; Abdelaziz, A.Y.; Hong, J.; Geem, Z.W. Optimal Planning of Multitype DGs and D-STATCOMs in Power Distribution Network Using an Efficient Parameter Free Metaheuristic Algorithm. *Energies* **2022**, *15*, 3433. https://doi.org/10.3390/en15093433

Received: 27 March 2022
Accepted: 6 May 2022
Published: 8 May 2022

1. Introduction

1.1. General

Within the power system structure hierarchy, power distribution networks (PDNs) are designed to deliver the electric energy produced by the central bulk generating stations to the customers through a web of transmission grids. However, for various reasons, including the widespread use of cables, undersized conductors, radial configuration, and inadequate reactive power support at the distribution level, the PDN is frequently accompanied by a poor voltage profile, an unstable operational mode, and excessive energy losses. Furthermore, the escalation in energy demand, soaring fuel costs, fast-depleting energy reserves, and global efforts to harvest clean and green energy have compelled the power distribution network operators (PDNO) to seek out alternative network planning approaches [1] to improve system performance while satisfying environmental and economic requirements. The distribution network planning (DNP) entails augmenting distributed generators (DGs) [2], reconfiguring the network topology (the process of changing the state of sectionalizing and tie switches) [3], compensating for reactive power [4], and combining these techniques [5,6]. Over time, DNP has evolved as a complex, combinatorial, and multi-objective optimization problem that aims to determine the optimal combination of planning approaches and optimal device allocation (DGs, reactive power compensating equipment), and to alter the status of switches (tie switches and sectionalizing switches) to meet the techno-economic and environmental requirements while adhering to several operating system constraints. As a result, optimal DNP necessitates efficient metaheuristic approaches [7].

Amidst the rise in fuel cost, the cost of energy production by the traditional generators has escalated. However, due to technological advancement, energy production by renewable sources, viz. solar and wind, is becoming more affordable [8]. This enforces the integration of renewable distributed generation on a wide scale into the existing grid. The incorporation of DGs can bring several opportunities to PDNOs not only in terms of improvement in the technical performance (power loss reduction, voltage profile enhancement, and acceptable voltage stability margin) of the system but also in terms of several economic (reduction in energy loss cost and deferral of system upgrade) and environmental benefits (reduction in greenhouse gas emissions). Nevertheless, the wrong assignment of DGs can be detrimental to the system. Therefore, DG deployment is challenging and strenuous for the PDNOs to reap all the benefits. As a result, the optimal allocation of DGs (OADG) requires an efficient optimization technique [2].

As the number of nonlinear loads in the PDN grows, reactive power shortage causes unacceptable voltage magnitude, resulting in voltage collapse. This can be solved through network reconfiguration (NR), allocation of shunt capacitors banks (SCBs), on-load tap changers (OLTC), and deployment of custom power devices (CPD). However, owing to the sluggish dynamic response and associated power quality issues, NR, SCBs, and OLTC are replaced by CPDs such as dynamic voltage restorers (DVRs), distribution static compensators (D-STATCOMs), and unified power quality conditioners (UPQCs) to ensure safer and quality power delivery to the end users [9]. A voltage source converter-based D-STATCOM is a shunt-connected controller that offers rapid reactive power exchange with a smooth operational performance. D-STATCOM is most favored for reactive power management in the PDN as it comes with low cost, compact size, less harmonic injection, and simple control algorithms [9,10]. Optimal allocation (location and capacity) of D-STATCOMs can assure their effective utilization.

1.2. Related Works

Considering the plethora of advantages that DGs can offer, various methods are suggested by preceding researchers to augment DGs into the PDN to improve system performance. The presence of continuous and discrete decision variables, nonlinear objective functions, and various operational constraints have made the OADG problem a complex optimization problem. Different heuristic, analytical, metaheuristic, and hybrid methods are proposed to solve the OADG problem [11]. Different versions of the improved stochastic fractal search algorithm (iSFSA), which is the combination of the original fractal search algorithm embedded with 10 different chaotic maps, are used to select the best sizes and locations for inserting DGs into the PDN for minimizing the real power loss (RPL) [12]. The optimal number of DGs are then selected after comparing the results of OADG obtained for different numbers of DGs. Authors in [13] have proposed a new hybrid multiverse optimization (HMO) algorithm to solve OADG in a multi-objective framework considering four different objectives, viz. energy loss, overall voltage deviation (OVD), overall voltage stability margin (OVSM), and energy not served (ENS). The said objectives are combined to formulate the multi-objective function (MOF), where the weights associated with each objective are determined using the analytical hierarchy process (AHP). An adaptive equilibrium optimizer (AEO) [14] is used to efficiently allocate biomass-based DGs to simultaneously reduce polluting gas emissions, minimize annual energy loss costs, and maximize surplus energy sales profits. A quasi-oppositional chaotic symbiotic organisms search (QOCSOS) is suggested in [15] to optimally allocate DGs operating at unity and non-unity power factors to improve the technical performance (RPL, voltage deviation, and voltage stability index) of the system. Simultaneous sizing and placement of unity power factor (UPF) DGs are investigated in [16] using a novel manta ray foraging optimization (MRFO) algorithm to diminish RPL considering the different number of DGs. The research suggested that the allocation of three DGs has resulted in maximum RPL minimization. A hybrid approach, which is the joint execution of a genetic algorithm (GA) and stain bowerbird optimization (SBO), is developed in [17] for solving OADG in a multi-objective formulation consisting of RPL, VD, emission, and costs associated with power import from the grid and fixed and variable costs of the DGs. The effect of the allocation of DGs in a reconfigured network is analyzed in [18], considering an improved equilibrium optimization algorithm (iEOA).

DNP considering optimal deployment of D-STATCOMs are envisaged in several works of literature. Yuvraj et al. [19] have presented a method to determine the optimal capacity of D-STATCOM using the bat algorithm (BA) at a predetermined location (obtained by voltage sensitivity index) to diminish the RPL. Ant colony optimization (ACO)-based D-STATCOM allocation is proposed in [20] to minimize the real power loss RPL, voltage deviation (VD), and installation, operation, and annual maintenance costs. In [21], a gravitational search algorithm (GSA) is used to optimally allocate D-STATCOM units to minimize RPL, VD, and annual energy loss (AEL) costs. Authors in [22] have obtained an optimal rating of D-STATCOM using a whale optimization algorithm (WOA) to reduce RPL and improve the voltage profile where the optimal injection node for D-STATCOM is obtained using a voltage stability index (VSI). A nature-inspired cuckoo search optimization (CSO) technique is presented to assign optimal D-STATCOM units to minimize RPL considering different load models viz commercial, residential, and industrial loads [23]. DNP considering the optimal allocation of D-STATCOM using a differential evolution algorithm (DEA) is carried out in [24] to minimize the RPL and maximize savings. A modified sine cosine algorithm (mSCA) is proposed to simultaneously optimize the placement and capacity of multiple D-STATCOM units to curb RPL and VD [25]. Considering discrete values for locations and continuous values for the size of D-STATCOMs, a discrete-continuous version of GA is proposed in [26] to optimally allocate D-STATCOMs for minimizing annual energy loss cost and annual investment cost while considering industrial, residential, and commercial load profiles. An improved bacterial foraging algorithm (iBFA) is proposed to solve the optimal placement and sizing of a single D-STATCOM unit to reduce RPL, minimize VD, and improve VSI [27].

Though some researchers dealt with optimal DNP considering DGs [11–18] and D-STATCOMs [20–27] separately, it is interesting to analyze the system performance considering the simultaneous allocation of DGs and D-STATCOMs. A novel multi-objective approach based on a lightning search algorithm (LSA) is proposed in [28] to allocate DGs and D-STATCOMs considering linear variation in feeder load from 50% to 160%. Later, a curve-fitting technique (CFT) is applied to determine the optimal sizes of the devices for different load levels. A nature-inspired cuckoo search algorithm (CSA) is applied for simultaneous optimal assignment of DGs and D-STATCOMs in a multi-objective mathematical formulation [29]. A modified flower pollination (mFP) approach is proposed in [30] to optimally place D-STATCOM and photovoltaic DGs simultaneously in a multi-objective formulation consisting of RPL minimization, load balancing index minimization, and maximization of voltage profile improvement. The VSI predetermines the photovoltaic (PV) DG and D-STATCOM insertion buses. A novel whale optimization algorithm (WOA) is proposed to simultaneously allocate DGs and D-STATCOMs at buses predetermined by a loss sensitivity factor (LSF), aiming to minimize the RPL and operating cost of devices [31]. Authors in [32] have applied a hybrid firefly algorithm (FA) and particle swarm optimization (PSO) algorithms for optimal allocation of PV-DGs and D-STATCOMs, considering several technical, economic, and environmental indices in a multi-objective framework. The optimal rating and placement of DGs and D-STATCOMs are computed using a hybrid lightning search (LS) and simplex method (SM) and LSF, respectively, to arrest the RPL of the PDN [33]. Simultaneous optimal sizing and sitting of PV-DGs and D-STATCOMS considering uncertainties associated with solar irradiance and the system load is addressed using a modified ant lion optimizer (MALO) [34]. Simultaneous allocations of DGs and different shunt compensators (SCs), viz. SCB, static var compensator (SVC), and D-STATCOM, are envisaged using a bald eagle search (BES) in [35] to curb RPL. The effect of simultaneous allocation of DGs and SCs on the PDN is studied in terms of RPL, reactive power loss, total VD, and stability index, both with and without allocation of devices. In [36], optimal DNP is investigated for simultaneous allocation of PV-DGs with battery energy storage and D-STATCOMs. A joint allocation of DGs and D-STATCOMs combined with NR is discussed in [37] to minimize RPL, improve feeder load balancing and arrest VD using ant colony optimization combined with a fuzzy multi-objective approach.

As previously mentioned, metaheuristic techniques are becoming more popular for solving exclusive OADG, exclusive D-STATCOM allocation (OADS), and simultaneous DG and D-STATCOM allocations (SOADGDS). The recently proposed student psychology-based optimization (SPBO) technique [38] is based on the psychology of students striving to be the best student by continuously improving their class performance. The algorithm's key benefit is that it lacks any algorithm-specific parameters (ASPs). As a result, it can be used to tackle any optimization problem without worrying about tuning its ASPs. Furthermore, the supremacy of the SPBO algorithm over 10 state-of-the-art metaheuristic approaches, including PSO [39], teaching learning-based optimization (TLBO) [40], cuckoo search algorithm (CSA) [41], symbiotic organism search [42], success-history-based adaptive differential evolution (SHADE) [43], and grey wolf optimization (GWO), [44] has been established by comparing the results on CEC 2015 benchmark functions in [38]. Authors in [45,46] have suggested the SPBO algorithm to solve the OADG problem. Another parameter-free metaheuristic (PFM) optimization technique, a symbiotic organism search (SOS) [42], follows the various symbiotic relationships that occur between organisms in an environment to enhance their survival chances. After being used to tackle a variety of real-world engineering challenges, SOS has evolved into a global optimizer. The SOS's improved performance comes from balancing exploration and exploitation without the use of algorithmic parameters [47]. Harris hawk optimization [48] is yet another recently proposed PFM optimization approach for solving real-world optimization problems.

1.3. Motivations

In light of the above discussion, it is observed that the DNP, which involves allocation of exclusive devices [11–27] to a combination of devices [28–37], can be framed as a single objective [12,16,19,23,25,35] or a multi-objective [11,13–15,17,20–22,24,26–34,36,37] optimization problem, and can have fewer decision variables [11–27] or a fairly large number of decision variables [28–37], and nonlinear objective function(s). Furthermore, the decision variables may be binary (on or off), discrete (location of devices), or continuous (sizes of devices), or any mix of the three. The penetration limit of DGs is always increasing as technology advances. It reduces grid real-power import, resulting in a poor power factor. Therefore, as DG penetration increases, the amount of reactive power compensation required also increases proportionately. Hence, the constraints on the sizes of DGs and D-STATCOMs are dynamic and flexible. As an exception, NR has strict radiality and topological constraints [3]. Therefore, other DNP regimes, except for NR, do not have a known global optimum.

Furthermore, complying with the "no free lunch theorem" [49], several metaheuristic algorithms have recently been proposed to solve complex engineering problems. Power system engineers are implementing different optimization algorithms [7,9–37,45,46] to search for the optimal solution to DNP. Despite the non-iterative feature of the analytical approaches, metaheuristic approaches are getting widespread attention for solving DNP problems simply because metaheuristic approaches are flexible and efficient in handling combinatorial optimization problems [7,11]. A compact review of the recently proposed metaheuristic approaches implemented to solve OADG, OADS, and SOADGDS are presented in Table 1.

Table 1. Summary of related works.

Ref.	Year	Planning Approach	Methods	Objective Function	Number of ASPs	Selection of Weights in the MOF	Review Remarks
[7]	2021	OADG	Different PSO variants	Cost and Emission	Refer [7]	$w_1 = 0$, $w_2 = 1$ $w_1 = 1$, $w_2 = 0$ $w_1 = 1$, $w_2 = 1$	Technical factors are not considered. For MOF, both objectives are given equal priority. Results revealed that hierarchical PSO has performed better.
[12]	2018	OADG	iSFSA	RPL	Maximum diffusion number = 5	-	OADG is solved considering single objective only The results are compared with SFS and PSO. The control parameters of PSO are determined experimentally.
[13]	2019	OADG	HMO	Energy Loss, OVD, OVSM, ENS	Wormhole existence probability = 0.2–1.0 Control parameter (m) = 0.5 Maximum chaotic iterations = 20	AHP $w_1 = 0.3940$ $w_2 = 0.2593$ $w_3 = 0.1970$ $w_4 = 0.1497$	AHP is adopted to decide the optimal values of weights in the MOF. DGs operating at UPF and non-unity power factor (N-UPF) are considered. Too many control parameters to be tuned.
[14]	2021	OADG	AEO	Benefits and cost of utility	Generation rate control parameter (Gp) = 0.5, Constant related to exploration ability (a_1) = 2 Constant related to exploitation ability (a_2) = 1	-	Results are compared with GWO, RAO, and DE. Biomass DGs are considered. Too many control parameters to deal with. Technical parameters are not included in the objective function (OF).
[15]	2020	OADG	QOCSOS	RPL, VD, 1/VSI	Jumping rate (Jr) = 0.4	$w_1 = 1$ $w_2 = 0.6$ $w_3 = 0.35$	Weights in the OF are subjectively assigned. DGs operating at UPF and N-UPF are considered. Missing economic analysis.
[16]	2021	OADG	MRFO	RPL	Somersault factor (SF)	--	The performance of the MRFO is highly sensitive to the number of search agent, maximum iteration and SF. Only single objective is considered.
[17]	2021	OADG	Hybrid GA-SBO algorithm (H-GASBO)	RPL, VD, Emission, Cost	Greatest step size(α) = 0.94 Mutation probability(p) = 0.05 Percent of the difference between the upper and lower limit (Z) = 0.02	NR	Too many control parameters to be tuned. MOF considers, technical, economic and emission factors.
[18]	2020	OADG and NR	IEO	TPL, 1/TVSI	a1 = 2 a2 = 1 Generation probability (G_P) = 0.5	$w_1 = 0.7$ $w_2 = 0.3$	Weights in the OF are subjectively assigned. Too many control parameters to be tuned. Economic factor is missing in the MOF.
[19]	2017	OADS	BA	RPL	Loudness = 0.5 Pulse rate = 0.5	-	Considers minimization of the RPL only.

[20]	2018	OADS	ACO	RPL, VD, Cost	α = 1 β =2	w_1 = 0.5 w_2 = 0.3 w_3 = 0.2	Weights used to combine multiple objectives are randomly selected. The values of control parameters are not tunned.
[21]	2019	OADS	GSA	RPL, VD, AEL costs	NR	w_1 = 1 w_2 = 1 w_3 = 1	Allocation of single D-STATCOM unit is considered. All objectives are given equal importance.
[23]	2020	OADS	CSO	RPL	2 (Discovery rate of alien egg, Pa = 0.25, Dimension Search Space = 1or 3)	-	LSF is used to identify the D-STATCOM insertion buses. Empirical analysis is conducted to determine the optimal parameter setting. Only single objective is considered.
[24]	2020	OADS	DE	Total energy loss cost and total cost of D-STATCOM)	Crossover rate (Cr) = 0.8 Scaling factor (F) = 1	Penalty factors are set at 0.1 for both the objectives.	Penalty factor is used to handle the constrained optimization problem. Single D-STATCOM is allocated.
[25]	2021	OADS	mSCA	RPL	a = 2	-	Considers minimization of the RPL only.
[26]	2021	OADS	DC-GA	Annual cost function of energy losses and annualized investment cost	NR	NR	Placement and sizing of the D-STATCOM are obtained by the discrete and continuous part of the codification respectively. Technical factors are not considered in the OF
[27]	2021	OADS	iBFA	PL, VD, $1/VSI_k$	Run-length unit Step size	w_1 = 0.5 w_2 = 0.25 w_3 = 0.25	Allocation of single D-STATCOM unit is considered. Weights in the MOF are subjectively assigned. Economic factor is not considered in the MOF.
[28]	2017	OADGDS	LSA	RPL, TVD, VSI	Maximum channel time	w_1 = 0.4 w_2 = 0.3 w_3 = 0.3	Optimal allocation of DG and D-STATCOM are carried out by varying feeder loads linearly in the range 0.5 to 1.6. Weights in the MOF are subjectively assigned. Economic factor is not considered in the MOF
[29]	2018	OADGDS	CSA	RPL and Cumulative voltage deviation (CVD)	Discovery rate of alien egg = 0.25 Dimension search space = 1or 3	w_1 = 0.7 w_2 = 0.3	VSI and LSF are used to pre locate DG and D-STATCOM injection buses respectively. CSA is used to determine the size of the devices. Weights in the MOF are subjectively assigned. Economic factor is not considered in the MOF.
[31]	2019	OADGDS	WOA	RPL, Operating cost of DGs and D-STATCOMs	Linearly decreasing weight (a) = 2 Coefficient describing spiral shape (b)	w_1 = 0.6 w_2 = 0.4	Location is obtained through LSF and size by WOA. Weights in the MOF are subjectively assigned.
[32]	2021	OADGDS	Hybrid FA with sine co-	RPL level, short circuit level, VD	C_{min} = 0.5 C_{max} = 2.5; α = 1/3; c_{1i} = 2.5 c_{1f} = 0.5,	w_1 = 0.3 w_2 = 0.2 w_3 = 0.2	The values weights in the MOF are based on practical indicators.

			sine acceleration coefficients PSO	level, Net Saving level, environmental pollution reduction level	c_{2i} =0.5 c_{2f} = 2.5; c_i =0.5 c_f = 2.5; ∂ = 2, $\eth$ = 0.5	w_4 = 0.2 w_5 = 0.1	
[33]	2021	OADGDS	Hybrid LS-SM optimization algorithm	PL, VD, TOC	Not Reported	w_1 = 0.5 w_2 = 0.25 w_3 = 0.25	LSF is used to identify the DG & D-STATCOM insertion buses. Simplex method and elite opposite-based learning is incorporated to improve the performance of LSA. Weights in the MOF are subjectively assigned.
[34]	2021	OADGDS	MALO	cost reduction, VD minimization, and VSI enhancement	A_{max} = 0.85 A_{min} = 0.4	NR	Levy Flight is used to enhance the exploration of the basic ALO algorithm. Variation in solar irradiance and the load are considered for solving the OADGDS.
[35]	2022	DGs & SRC	BES	RPL	c_1, c_2, r, α	-	Only single objective is considered. Too many control parameters. Different SRC viz, SCB, SVC & D-STATCOM are considered

As noted in Table 1, several metaheuristic approaches are applied for solving multi-objective combinatorial optimization problems like optimal DNP. However, most metaheuristic approaches require certain control parameters to balance the exploration and exploitation to yield an optimal solution. The selection of these control parameters is quite tedious and has a substantial impact on the algorithm's performance. Therefore, recently, parameter-free metaheuristic (PFM) optimization techniques have been proposed. The student psychology-based optimization (SPBO) technique is a PFM algorithm proposed by Das et al. [27] that is based on the psychology of students to continuously perform better in their class performance. The authors in [27] also proved the supremacy of the SPBO algorithm over 10 state-of-the-art metaheuristic approaches by comparing the results of the CEC 2015 benchmark functions. Exclusive allocation of DGs using SPBO is proposed in [28]. The symbiotic organism search [29] is another PFM optimization technique that follows the various symbiotic relationships existing between organisms of an ecosystem to improve their survival opportunities. After being used to tackle a variety of real-world engineering challenges, SOS has evolved into a global optimizer. Enhancement in SOS's performance is due to its capacity to strike a balance between exploration and exploitation without using algorithmic parameters [30]. The Harris hawk optimization [31] is yet another recently proposed PFM optimization approach for solving real-world optimization problems.

Most metaheuristic techniques have ASPs, as shown in Table 1, and tuning these parameters introduces a new subproblem, increasing the computing cost. Furthermore, the appropriate ASP values significantly impact the quality of the optimal solution. As a result, PFM algorithms are logical for dealing with the DNP. VSI [29] and LSF [23,31,33] are two sensitivity techniques that a few researchers have utilized to identify the prospective locations for the deployment of the devices. The device's ideal rating is then calculated using several metaheuristic methods. Technical, economic, and environmental considerations must all be taken into account for a comprehensive and pragmatic optimal DNP. However, authors in [12,16,19,23,25,35] have established a single goal for addressing the optimal DNP. Few authors have looked at only the technical [13,15,18,27,28], the solely economic [14,24,26], or both the technical and economic aspects [20,21,31,33,34]. However, [17,32] authors took technical, economic, and environmental concerns into account. The weighted sum multi-objective (WSMO) strategy is one of the most prominent approaches for combining multiple objectives. In the WSMO technique, each objective is given a weight and the values allocated to these weights are crucial in determining the overall objective function. As a result, selecting the most appropriate weight for each objective function is critical. However, except when the PDNO's perspective and expertise are taken into account, these weights are usually picked at random. Lastly, most researchers have suggested DGs be powered by solar, wind, or biomass instead of having mixed energy sources.

1.4. Contribution

In the light of the above discussion, the major contributions of the current manuscript are outlined below.

- Three recently surfaced parameter-free metaheuristic algorithms, viz. the student psychology-based optimization, symbiotic organism search optimization, and Harris hawk optimization, are implemented for optimal planning of a power distribution network.
- Optimal allocations of seven different combinations of PV-DGs, gas-turbine-based DGs, and D-STATCOMs are studied.
- Optimal planning combines technical, economic, and environmental indices using suitable weights derived from the analytical hierarchy process.

1.5. Manuscript Organisation

The paper is organized as follows: modeling of devices, viz. solar photovoltaic (PV) DGs, gas-turbine (GT) DGs, and D-STATCOMs are included in Section 2. Section 3 formulates the weighted-sum-based multi-objective simultaneous allocation problem of DGs and D-STATCOMs using four indices. Three parameter-free metaheuristic (PFM) approaches are introduced in Section 4. In Section 5, the implementation of PFM to solve simultaneous OA-DG-DS problems is elucidated. Results and discussions are presented in Section 6 followed by the conclusions in Section 7.

2. Modeling of Devices

In this paper, the optimal planning of multitype DGs, viz. solar PV-DGs, gas-turbine DGs (GT-DG), and D-STATCOMs is carried out. A simplified two-node equivalent of a DN connected to DGs and a D-STATCOM is shown in Figure 1. A brief modeling aspect of solar PV-DG, GT-DG, and D-STATCOM is discussed below.

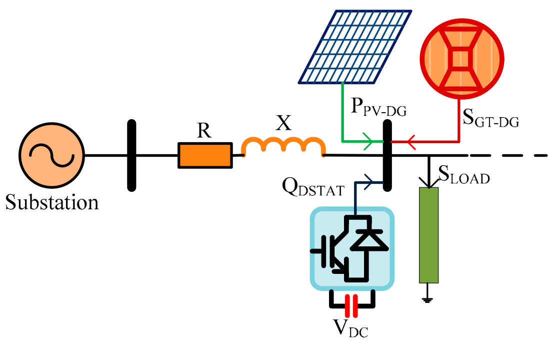

Figure 1. A simplified two-node equivalent of a DN connected to DGs and DSTATCOM.

2.1. Solar Photo Voltaic DG

The output power of the solar photovoltaic DG (PV-DG) is sensitive to the panel characteristics and meteorological conditions of the site. Due to the intermittent nature of the power produced by PV-DG, it is treated as a non-dispatchable DG. The following sets of Equations (1)–(5) [32] are used to attribute the power generated by the PV-DG.

$$T_c = T_a + S\left(\frac{N_{OT} - 20}{0.8}\right) \tag{1}$$

$$I_k = S\left[I_{sc} + K_i (T_c - 25)\right] \tag{2}$$

$$V_k = V_{oc} - K_v T_c \tag{3}$$

$$FF = \frac{V_{MPP} \times I_{MPP}}{V_{oc} \times I_{sc}} \tag{4}$$

$$P_{PV} = N \times FF \times V_k \times I_k \tag{5}$$

where T_c, T_a, and N_{OT} represent the cell temperature, ambient temperature, and nominal cell operating temperature, respectively. K_i and K_v are the temperature coefficients for current and voltage, respectively. Voltage and the current during maximum power point are designated as V_{MPP} and I_{MPP}, respectively. I_{SC} and V_{OC} are the short-circuit current and the open-circuit voltage, respectively, of the *PV* panel. *N* is the number of *PV* panels in use and *FF* is the fill factor of the *PV* panels. Voltage and current of the *PV* panel are denoted as V_k and I_k, respectively. An inverter-based SPV-DG can operate in lagging power factor mode, which allows the DG to inject reactive power into the grid in addition to real power. The reactive power injected by the PV-DG can be exposed as:

$$Q_{PV} = P_{PV} \times \tan(\phi) \tag{6}$$

where ϕ is the power factor angle.

2.2. Gas Turbine DG

Gas-turbine-based DGs (GT-DGs) are attracting widespread attention as they offer higher operational efficiency (close to 80%), leave a smaller carbon footprint, and support a dispatchable mode of operation. They can also be utilized for cogeneration to provide combined heat and power. In GT-DGs, highly pressurized natural gas is used for energy conversion and its output power can be controlled by regulating the amount of natural gas supplied as the input fluid. Therefore, deterministic models are used to represent the GT-DGs. Furthermore, by connecting a suitable power electronics interface between the DG and the load, it can be operated at a lagging power factor.

2.3. D-STATCOM

D-STATCOM is a sophisticated device connected at the distribution voltage level to facilitate fast reactive power exchange for alleviating power quality issues. In the present work, a steady-state model of D-STATCOM is developed that can be used to study the steady-state impact of D-STATCOM on the DN. Consider a D-STATCOM connected to the $(t+1)^{\text{th}}$ node (receiving node) of DN, as shown in Figure 1. This will modify the voltage of the corresponding node as:

$$U'_{t+1}\angle\theta'_{t+1} = U'_t\angle\theta'_t - \left(R_m + jX_m\right)\times I_m\angle\delta_m - \left(R_m + jX_m\right)\times(I_{DSTATCOM}\angle\psi) \tag{7}$$

To exchange reactive power, the current supplied by the D-STATCOM and the compensated node voltage must maintain a 90-degree phase difference. Therefore:

$$\psi = \frac{\pi}{2} + \theta'_{t+1} \quad (8)$$

So, the rating of the D-STATCOM can be obtained as:

$$-jQ_{DSTATCOM} = U'_{t+1}\angle\theta'_{t+1} I^{*}_{DSTATCOM}\angle\left(\frac{\pi}{2} + \theta'_{t+1}\right) \quad (9)$$

where $Q_{DSTATCOM}$ and $I_{DSTATCOM}$ represent the reactive power delivered and current supplied by the D-STATCOM at $(t + 1)^{th}$ bus, respectively.

3. Problem Formulation

A simultaneous optimal allocation of DGs and D-STATCOM (OA-DG-DS) for a power distribution system is formulated considering the following indices for the overall performance enhancement of the system [33].

3.1. Real Power Loss Minimization Index (RPLMI)

Active power loss (APL) minimization is considered the most significant objective to improve the performance of the DN. Therefore, the effect of the allocation of DGs and D-STATCOMs (devices) on APL reduction must be assessed. *RPLMI* is the ratio of the APL of the system with and without allocation of the devices. It is formulated to quantify the impact of device (DGs and D-STATCOMs) installations on APL minimization of the DN.

$$RPLMI = \frac{PLOSS^{device}}{PLOSS^{base}} \quad (10)$$

where $PLOSS^{base}$ is the base case power loss (i.e., without allocation of any devices), and the APL of the system in the presence of devices is designated as $PLOSS^{device}$. Equation (11) can be used to determine the system APL.

$$PLOSS = \sum_{m=1}^{nbus} \left|I_m\right|^2 \times R(m) \quad (11)$$

An *RPLMI* having a unity value corresponds to no effect of the device allocation on APL minimization of the DN. A positive effect of device allocation is marked by an *RPLMI* value less than unity. An *RPLMI* value more than unity corresponds to an increase in the system's APL in the presence of the devices and therefore is viewed as a negative system impact.

3.2. Bus Voltage Variation Minimization Index (BVVMI)

DNs being radial experience a wide variation of the bus voltage. The fluctuation in bus voltage gets more pronounced as the location of the bus goes farther from the substation. If the bus voltage variation is not maintained within a prescribed limit, it can lead to detrimental system performance. The effectiveness of device allocation on voltage profile enhancement can be observed using the bus voltage variation minimization index (*BVVMI*) as:

$$BVVMI = \frac{VD^{device}}{VD^{base}} \quad (12)$$

The VD^{base} denotes the voltage deviation *(VD)* of the base case scenario, whereas the *VD* of the *DN* in the presence of devices is represented by VD^{device}. Equation (13) is employed to determine the *VD* of the *DN*.

$$VD = \sum_{i=1}^{nbus} (U_i - U_s)^2 \tag{13}$$

where U_s and U_t are the substation and the bus voltage magnitude, respectively.

A *BVVMI* having a unity value corresponds to no effect of the device allocation on the bus voltage variation. A positive effect of device allocation is marked by a *BVVMI* less than unity. A *BVVMI* value more than unity is reflected as a negative system impact in the presence of the devices.

3.3. System Voltage Stability Maximization Index (SVSMI)

An increased percentage of sensitive and nonlinear loads into the DN requires fast and adequate reactive power support for maintaining secure and stable network operation. Lack of reactive power support may force the DN into the insecure mode of operation, leading to system blackouts. Installation of DGs (operating in lagging power factor mode) and D-STATCOMs can significantly improve the secure operation of the DN. In this regard, the voltage stability index (VSI) [34] of the DN can be computed using Equation (14) to access the state of the security and stability of the network.

$$VSI(t+1) = |U_t|^4 - 4\left[P_{t+1}^{eff} \times X_m - Q_{t+1}^{eff} \times R_m\right]^2 - 4\left[P_{t+1}^{eff} \times R_m + Q_{t+1}^{eff} \times X_m\right]|U_t|^2 \tag{14}$$

where P_{t+1}^{eff} and Q_{t+1}^{eff} represent the effective active and reactive load demand for *(t* + 1) bus, respectively. Furthermore, R_m and X_m are resistance and reactance, respectively, of the branch connecting the *t* and *t + 1* buses.

A *VSI* closer to unity indicates better system stability, whereas a *VSI* closer to zero indicates an unstable system operating mode. The bus corresponding to the least *VSI* value of the DN is called a critical bus. Therefore, a system voltage stability maximization index (SVSMI) is developed using Equation (15), as the ratio of the reciprocal of the voltage stability index of the DN's critical bus with and without device consideration to assess the influence of device allocation on the stability margin.

$$SVSMI = \frac{1/VSI_c^{device}}{1/VSI_c^{base}} \tag{15}$$

The values of *SVSMI* can be less than unity, equals unity, or more than unity. Allocation of devices will be considered beneficial for an *SVSMI* value less than unity as it corresponds to a value of *VSI* of the critical bus closer to unity in the presence of the devices compared to the DN without devices.

3.4. System Annual Cost Minimization Index (SACMI)

When no devices are installed in the DN, the distribution utility (DU) has to meet the annual cost of purchasing power from the upstream grid and leverage the penalty for emissions caused by the outsourced power from the thermal stations. Equation (16) shows clearly how much DUs pay each year in the base case.

$$AC^{base} = P_{sub}^{base} \times k_{sub}^{real} \times 8670 + Q_{sub}^{base} \times k_{sub}^{reac} + k_{em}^{sub} \times P_{sub}^{device} \times 8670 \times E_{grid} \tag{16}$$

However, when different devices are introduced, the capital cost and operation and maintenance cost of the devices has also to be shared by the DU as formulated in (17).

$$AC^{device} = C^{device} + P_{sub}^{device} \times k_{sub}^{real} \times 8670 + Q_{sub}^{device} \times k_{sub}^{reac} + k_{em} \times P_{sub}^{device} \times 8670 \times E_{grid} + k_{em} \times P_{DG} \times 8670 \times E_{DG} \tag{17}$$

$$C^{device} = \frac{IC^{device}}{LS^{device}} + OM^{device} \tag{18}$$

However, in the presence of the devices, energy purchase cost and emission cost will be significantly reduced, causing the net annual cost to be substantially less than that without the installation of devices.

The impact of device allocation on the annualized cost borne by the DU is measured by the system annual cost minimization index (*SACMI*), which is defined as the ratio of the annual cost borne by DU with and without the allocation of devices.

$$SACMI = \frac{AC^{device}}{AC^{base}} \tag{19}$$

3.5. Multi-Objective Function(MOF)

The allocation of the individual and a combination of devices can significantly affect the performance of the DN by diminishing power loss, boosting the voltage profile, and enhancing the stability margin. Moreover, in the deregulated framework, the owners of the devices must earn economic benefits, which incentivize them to invest in sophisticated devices. Therefore, the allocation of the devices must be envisaged to ensure the technical and economic benefits. Hence, considering the above facts, both the technical factors, viz. APLRI, VDMI, and VSII, and the economic factor ACMI are suitably combined to formulate the multi-objective function as exposed in Equation (20).

$$MOF = \min(w_1 RPLMI + w_2 \times BVVMI + w_3 \times SVSMI + w_{4.} \times SACMI) \tag{20}$$

where w_1, w_2, w_3, and w_4 are the constants that can be adjusted to prioritize the influence of individual factors on the overall *MOF*. The values of these weights are finalized using an AHP, as described below.

3.6. Analytical Hierarchy Process (AHP)

An AHP requires a priority matrix (*PM*) formulated up front to capture the pair-wise significance between the considered multiple-objective functions. PM is a square matrix with rows equal to the number of objective functions (*NOF*). Elements of each row of the PM signify the relative importance of each objective function compared to the other objective functions. The degree of importance is represented on a scale from 1 to 9, with 1 meaning both objectives are of equal importance and 9 meaning the concerned objective function is highly significant compared to the other objective functions. The formation of a PM is often guided by the expertise and requirement of the decision maker. The present work considers the following PM.

$$K = \begin{bmatrix} 1 & 3 & 6 & 9 \\ 0.3333 & 1 & 2 & 3 \\ 0.1667 & 0.5 & 1 & 1.5 \\ 0.1111 & 0.3333 & 0.6667 & 1 \end{bmatrix} \tag{21}$$

The rows of the PM represent RPLMI, BVVMI, SVSMI, and SACMI, respectively. It can be seen that the objective of power loss minimization is given the highest priority against the annual cost reduction, whereas it is made moderately significant as compared to the objectives of voltage deviation and voltage stability index, respectively. Furthermore, the voltage stability index objective is given more importance than the voltage deviation objective.

The suitable values of the weights can be computed from the PM (*K*) using the following equation.

$$w_i = \frac{\sqrt[N_{OF}]{\prod_{j=1}^{N_{OF}} k_{ij}}}{\sum_{i=1}^{N_{OF}} \sqrt[N_{OF}]{\prod_{j=1}^{N_{OF}} k_{ij}}} \quad (22)$$

Following the above process, the weights of the MOF are computed as $w_1 = 0.6207$, $w_2 = 0.2069$, $w_3 = 0.1034$, and $w_4 = 0.0690$.

4. Parameter-Free Metaheuristic (PFM) Algorithms

Population-based metaheuristic algorithms are inherently the most preferred approaches to solve the simultaneous optimal allocation problems, though they are usually computationally burdensome. Therefore, parameter-free metaheuristic algorithms are the natural choice of researchers for solving this class of problems. In this paper, three such parameter-free metaheuristic algorithms (SPBO, SOS, and HHO) are considered to solve the planning problem formulated in the previous section.

4.1. Student Psychology Based Optimization (SPBO)

Student psychology-based optimization (SPBO) begins with an initial population of the prospective solution vectors that represent the performance of N students of a class in D different subjects. The fitness of the initial population is determined by evaluating the objective function that resembles the overall marks secured by the students in the class examination. The students often try to enhance their overall class performance by securing better marks in each subject offered to them and trying to be the topper of the class. A student's performance in a subject is influenced by factors like the student's interests, motivation/incentives for the subject, efficiency, and capability of the student to handle the subject. Therefore, the entire class is divided into four groups of students based on the students' psychology to perform in the examination. Group-I represents the student with the highest overall marks in the examination. S/he is called the best student or topper of the class. A student who belongs to this group puts valiant efforts into each subject compared to any other student of the class to maintain his/her first position in the class. Therefore, the performance of Group-I students can be expressed as:

$$p_{best,j}^{k+1} = p_{best,j}^{k} + (-1)^{\alpha} \times rand \times \left(p_{best,j}^{k} - p_{rj}^{k} \right) \quad (23)$$

The updated and the previous performance of the best student in the j^{th} subject is represented as $p_{best,j}^{k+1}$ and $p_{best,j}^{k}$ respectively. p_{rj}^{k} denotes the past performance in the jth subject of a random student of the class. α is a switching parameter, which can assume a value of 0 or 1. *rand* is a random number in the range [0, 1] drawn from a normal distribution.

Students who have performed well in the respective subjects are subject-wise good students (SGS) and are placed in Group-II. Because of the stated factors, SGS, though performing well in a particular subject, might have average performance in some other subjects. Therefore, the selection of students to Group-II is a random process. Some students in Group-II may try to be in Group-I by endeavoring to undertaken similar efforts as the topper of the class, and their improvement in performance can be defined in (24).

$$p_{i,j}^{k+1} = p_{best,j}^{k} + rand \times \left(p_{best,j}^{k} - p_{i,j}^{k} \right) \quad (24)$$

Where $p_{i,j}^{k+1}$ and $p_{i,j}^{k}$ are the performances of the i^{th} student in the j^{th} subject in the k^{th} and $(k+1)^{th}$ iterations, respectively. Again, some SGS may apply effort that is more than the average effort of the class, as well as in line with the effort made by the best student. It can be modelled as in (25):

$$p_{i,j}^{k+1} = p_{i,j}^{k} + \left| rand \times \left(p_{best,j}^{k} - p_{i,j}^{k} \right) \right| + \left| rand \times \left(p_{i,j}^{k} - p_{avg}^{k} \right) \right| \tag{25}$$

where p_{avg}^{k} is the average class performance in a k^{th} iteration.

Students with average performance in a subject are included in Group-III and called subject-wise average students (SAS). Since students' psychologies are different for different subjects, they are randomly included in Group-III. These students may improve their overall performance, as mentioned in (26):

$$p_{i,j}^{k+1} = p_{i,j}^{k} + \left| rand \times \left(p_{avg}^{k} - p_{i,j}^{k} \right) \right| \tag{26}$$

Students who do not have any structured effort to improve their performance and often perform poorly in the class belong to Group-IV and are referred to as below-average students (BAS). BAS apply random efforts to the subject to improve their overall score and therefore their performance improvement can be expressed as in (27):

$$p_{i,j}^{k+1} = p_{j}^{\min} + \left[rand \times \left(p_{j}^{\max} - p_{j}^{\min} \right) \right] \tag{27}$$

Where $p_{j}^{\max}$ and $p_{j}^{\min}$ are the maximum and minimum marks of the j^{th} subject.

Here, the psychology of different students to continuously upgrade their class performances reflects the intrinsic philosophy of optimization. The step-by-step implementation procedure of the SPBO Algorithm 1 is illustrated below.

Algorithm 1 Pseudocode for SPBO algorithm

Input: Class size (N)
Maximum number of iterations (K_{max})
Number of design variables (D)
Upper and lower bound of the design variables

Output: Best solution (P^{best})

1. Randomly initialize the class performance uniformly spread within the upper and lower bound of the design variables.
2. Evaluate the objective function.
3. Select the best solution P^{best}.
4. Set the iteration counter: k = 1.
5. ***while*** k < K_{max}.
6.   ***for*** i = 1: D.
7.   ***for*** j = 1: N.
8.   ***if*** student belongs to Group-I.
9.   Update student performance using Equation (23).
10.   ***else if*** student belongs to Group-II.
11.   ***if*** rand < 0.5.
12.   Update student performance using Equation (24).
13.   ***else***.
14.   Update student performance using Equation (25).
15.   ***end if***.
16.   ***else if*** student belongs to Group-III.
17.   Update student performance using Equation (26).
18.   ***else***.
19.   Update student performance using Equation (27).
20.   ***end if***.
21.   ***end for***.
22.   Evaluate the objective function using current class.

```
        if current class is better than previous class.
            Update previous class with current class.
        end if.
    end for.
end while.
```

4.2. Symbiotic Organisms Search (SOS)

The symbiotic organisms search (SOS) is a promising search algorithm where the symbiotic interactions between heterogeneous organisms to produce better organisms continually showcases the natural optimization process. It begins with an ecosystem that represents a population of organisms as in (28):

$$OG = [OG_1 \; OG_2 \; OG_3 \; \ldots \; OG_N]^T \tag{28}$$

where N represents the size of the ecosystem and each organism shall have D components (equal to the no of the optimization variable) as in (29):

$$OG_i = [og_{i1} \; og_{i2} \; og_{i3} \; \ldots \; og_{iD}], \; (i = 1,2,3 \ldots N) \tag{29}$$

The degree of survival of individual organisms is obtained by the functional evaluation of the ecosystem. The ecosystem is then iteratively subjected to three phases of symbiotic relationships, viz. the mutualism phase, communalism phase, and parasitism phase, till the predefined maximum number of iterations is reached. The basic operations of the stated symbiotic phases are elucidated below.

4.2.1. Mutualism Phase

In this phase, both participating organisms get benefits from the relationship. Here, an individual organism OG_i fosters a mutualism interaction with another randomly selected organism OG_j ($i \neq j$) from the ecosystem as modeled in (28) and (29) and produces two new organisms. Depending on the better rate of survival of the current organisms, previous-generation organisms get replaced.

$$OG_i^{new} = OG_i + rand(0,1) \times \left(OG_{best} - MV \times Bf_1 \right) \tag{30}$$

$$OG_j^{new} = OG_j + rand(0,1) \times \left(OG_{best} - MV \times Bf_2 \right) \tag{31}$$

$$MV = mean(Bf_1, Bf_2) \tag{32}$$

where *rand* is a uniformly distributed random number in the interval [0, 1], and the benefit factors corresponding to individual organisms are represented by Bf_1 and Bf_2, respectively. Bf_1 and Bf_2 stochastically assigned a value of either one or two. The mutual vector (MV) mimics the mutualism interaction between the organisms involved.

4.2.2. Communalism Phase

A communalism relationship is one where one of the organisms benefits from the symbiotic relationship without affecting the other organism. So, for two organisms, OG_i and OG_j ($i \neq j$), drawn from the ecosystem, the communalism relationship is established, such that only OG_i gets benefits, whereas OG_j remains unaffected, as mentioned in Equation (33):

$$OG_i^{new} = OG_i + rand(-1,1) \times \left(OG_{best} - OG_j \right) \tag{33}$$

4.2.3. Parasitism Phase

In the parasitism interaction, one of the involved species referred to as a parasite benefits immensely, whereas the other one, referred to as a host, is subjected to sheer suffering. To model this interaction, at first, a parasite vector (PV) is generated by copying and randomly altering some variable of the carrier of parasite OG_i. Then the PV interacts with a randomly selected host organism OG_j. If PV has a higher rate of survival, then it replaces the host in the ecosystem.

The step-by-step implementation procedure of the SOS Algorithm 2 is elucidated below.

Algorithm 2 Pseudocode for SOS algorithm

Input:	Ecosystem size (N) Maximum number of iterations (K_{max}) Number of design variables (D) Upper and lower bound of the design variables
Output:	Best solution (OG^{best})

1. Randomly initialize the ecosystem within the upper and lower bound of the design variables.
2. Evaluate the objective function.
3. Select the best solution OG^{bes}.
4. Set the iteration counter: k = 1.
5. ***for*** k = 1: K_{max}.
6.   ***for*** *i* = 1: N.
7.   Perform mutualism phase using Equations (30)–(31).
8.   Update the ecosystem if the current organism is better than previous.
9.   Perform Communalism phase using Equation (33).
10.   Update the ecosystem if the current organism is better than previous.
11.   Perform parasitism phase.
12.   Update the ecosystem if the current organism is better than previous.
13.   ***end for***.
14. Update OG^{best}.
15. ***end for***.

4.3. Harris Hawk Optimization (HHO)

Harris hawks (HH) are the most intelligent raptors found in the deserts of North America. The cooperative predation activity of HH, which includes searching for prey, surprising the prey, and attacking the prey, curates the structure of the Harris hawk optimization (HHO). Here, the initial population of the solution represents the random placement of the hawks and the prey (rabbit) is designated as the best solution. The initial population is iteratively guided through three stages of the algorithm unless a stopping criterion is encountered. The three stages of the algorithm are stage-I, the exploration stage, stage-II, the transition between exploration and exploitation stage, and stage-III, the exploitation stage.

Stage-I: HH searches for the prey either by sitting on a tall tree to scan the desert or by following the locations of the gaggle (which are closer to the prey). Citing equal probability for the above two perching behaviors, HH may update their placements as exposed in (32):

$$HH^{k+1} = \begin{cases} HH_r^k - rand * \left| HH_r^k - 2 * rand * HH^k \right|; q \geq 0.5 \\ HH_{prey}^k - HH_{mean}^k - rand * \left(HH_{mean}^k + rand * \left(HH_{\max} - HH_{\min} \right) \right) q < 0.5 \end{cases} \quad (34)$$

where HH^{k+1} and HH^k represent in sequence the placement of *HH* in the $(k + 1)^{th}$ and k^{th} iterations. *a rand* is a random number in the interval [0, 1]. The placement of the rabbit is presented as HH^k_{prey}, HH^k_r and HH^k_{mean} represent the placement of a randomly selected *HH* and the average placement of the gaggle in the k^{th} iteration, respectively. The average placement of the gaggle can be computed as follows:

$$HH^k_{mean} = \frac{1}{N}\sum_{i=1}^{N} HH^k_i \tag{35}$$

Stage-II: The performance of any optimizer depends on its ability to shift from the exploration to exploitation phase swiftly. Stage-II of HHO presents the transition from the exploration to exploitation stage. During the hunting, the prey gets tired as its energy is utilized in escaping from the predator. The dynamics of escaping energy is modelled in (36):

$$E = 2E_0(1 - \frac{k}{k_{\max}}) \tag{36}$$

where k, k_{max}, and E_0 are the current iterations, maximum iteration, and initial energy, respectively.

$|E| > 1$ indicates the exploration, as the *HH* search for a different location to find the rabbit, whereas exploitation sets in for $|E| < 1$.

Stage-III: This stage models the interaction of *HH* and the prey (rabbit) as four different perching tactics displayed by the HHs. The following four perching scenarios are framed based on the rabbit's attempt to escape the hunt ($P_{prey} < 0.5$ implies the rabbit avoids the predation and $P_{prey} \geq 0.5$ implies the rabbit falls prey to the HH) and the dynamics of the escaping energy.

Scenario-1: Soft besiege ($|E| \geq 0.5$ and $P_{prey} \geq 0.5$).

The following equations model the soft besiege strategy.

$$HH^{k+1} = \Delta H^k - E * \left| J * HH^k_{prey} - HH^k \right| \tag{37}$$

$$\Delta HH^k = HH^k_{prey} - HH^k \tag{38}$$

$$J = 2 * (1 - rand) \tag{39}$$

Scenario-2: Hard Besiege ($|E| < 0.5$ and $P_{prey} \geq 0.5$).

Hard besiege can be modeled as follows:

$$HH^{k+1} = HH^k_{prey} - E\left| \Delta HH^k \right| \tag{40}$$

Scenario-3**:** Soft besiege with a progressive rapid dive ($|E| \geq 0.5$ and $P_{prey} < 0.5$).

The following equations model the soft besiege with a progressive dive of HH.

$$HH^{k+1} = \begin{cases} Y_1; f(Y_1) < f(HH^k) \\ Z_1; f(Z_1) < f(HH^k) \end{cases} \tag{41}$$

where:

$$Y_1 = HH^k_{prey} - E * \left| J * HH^k_{prey} - HH^k \right| \tag{42}$$

$$Z_1 = Y_1 + S * LD(D) \tag{43}$$

where D is the no of design variables, S is a random vector of length D, and LD is levy distribution.

Scenario-4**:** Hard besiege with progressive rapid dive ($|E| < 0.5$ and $P_{prey} < 0.5$).

Hard besiege with progressive dive of HH can be modeled as follows:

$$HH^{k+1} = \begin{cases} Y_2; f(Y_2) < f(HH^k) \\ Z_2; f(Z_2) < f(HH^k) \end{cases} \quad (44)$$

where:

$$Y_2 = HH^k_{prey} - E * \left| J * HH^k_{prey} - HH^k_{mean} \right| \quad (45)$$

$$Z_2 = Y_2 + S * LD(D) \quad (46)$$

The step-by-step implementation procedure of the HHO Algorithm 3 is presented below.

Algorithm 3 Pseudocode for HHO algorithm

Input:	Population size (N) Maximum number of iterations (K_{max}). Number of design variables (D) Upper and lower bound of the design variables
Output:	Best solution (HH_{prey})

1. Randomly initialize the positions of HH uniformly spread within the upper and lower bound of the design variables.
2. Evaluate the objective function.
3. Select the best solution HH_{prey}.
4. Set the iteration counter: k = 1.
5. ***for*** k = 1: K_{max}.
6.   ***for*** *i* = 1: N.
7.   Update E using Equation (36).
8.   ***if*** $|E| \geq 1$.
9.   Update the position of HH using Equation (34).
10.   ***else***.
11.   ***if*** $P_{prey} \geq 0.5$ and $|E| \geq 0.5$.
12.   Update the position of HH using Equation (37).
13.   ***elseif*** $P_{prey} \geq 0.5$ and $|E| < 0.5$.
14.   Update the position of HH using Equation (40).
15.   ***elseif*** $P_{prey} < 0.5$ and $|E| \geq 0.5$.
16.   Update the position of HH using Equation (41).
17.   ***elseif*** $P_{prey} < 0.5$ and $|E| < 0.5$.
18.   Update the position of HH using Equation (44).
19.   ***end if***
20.   ***end if***
21.   ***end for***
22. ***end for***.

5. Implementation of PFM Algorithms for Simultaneous OA-DG-DS Problem

In this work, the SPBO algorithm and the other two parameter-free optimization algorithms are used as tools to determine the optimal location and size of the devices (D-STATCOMs, PV-DGs, and GT-DGs) separately and concurrently to minimize the proposed MOF. The optimal planning of the DN considers the following eight cases:

Case-1: DN without allocation of any devices;
Case-2: DN with exclusive D-STATCOMs allocation;
Case-3: DN with exclusive PV-DGs allocation;
Case-4: DN with exclusive GT-DGs allocation;

Case-5: DN with simultaneous D-STATCOMs and PV-DGs allocation;
Case-6: DN with simultaneous D-STATCOMs and GT-DGs allocation;
Case-7: DN with simultaneous D-STATCOMs with 2 PV-DGs and 1 GT-DG allocation;
Case-8: DN with simultaneous D-STATCOMs with 1 PV-DG and 2 GT-DGs allocation.

In the present work, DGs are operated at a combined load-power factor. Allocation of DGs is accomplished by considering these as negative loads at the respective candidate buses. Similarly, for D-STATCOM allocation, its equivalent current is subtracted from the corresponding bus current. A common approach is proposed to solve the OADGDS problem using the three PFM algorithms, as explained in the subsequent sections for the abovementioned cases.

5.1. Initialization

The initial population contains N individuals and each individual has D components. Each individual (X_i) corresponds to a potential solution vector to the optimization problem. The composition of the solution vector shall vary depending on the optimal planning strategy. For case-2, case-3, and case-4, the solution vectors shall contain sizes of the three individual devices (D-STATCOMs, PV-DGs, or GT-DGs) followed by their location strings, which are generated using Equation (45). Similarly, for the remaining cases, the solution vector shall contain sizes of the six individual devices (combination of D-STATCOMs, PV-DGs, and GT-DGs as per the cases) followed by their location strings, which are generated using Equation (48).

$$X_i = \left[size_{device1}, size_{device2}, size_{device3}, loc_{device1}, loc_{device2}, loc_{device3}\right] \tag{47}$$

$$X_i = \left[size_{device1}, \ldots, size_{device6}, loc_{device1}, \ldots, loc_{device6}\right] \tag{48}$$

These solutions are randomly generated within the stipulated ranges of the devices, as mentioned in Table 1, to be equally distributed throughout the whole solution space as defined by Equations (47) and (48).

$$size_{device} = size_{device,\min} + rand\left(size_{device,\max} - size_{device,\min}\right) \tag{49}$$

$$loc_{device} = round\left(loc_{device,\min} + rand\left(loc_{device,\max} - loc_{device,\min}\right)\right) \tag{50}$$

It is to be noted that each optimization technique uses different metaphors to refer to the population, best solution vector, etc. For example, the initial population or the solution vector in SPBO, SOS, and HHO are called a class, an ecosystem, and placements of hawks, respectively, where each individual may be termed as the performance of the student (as in SPBO), an organism (as in SOS), or position of the Harris hawk (as in HHO). Similarly, the best solution vector of the algorithm is known as the performance of the best student, best organism, and position of the prey (rabbit) in SPBO, SOS, and HHO, respectively.

5.2. Updation

The generated initial population for the respective planning schemes is then iteratively updated to yield the best planning solution unless the stopping criteria are met. However, each optimization technique employs its own mechanism to update the initial population. For example, in SPBO, the initial population is first subjected to functional evaluation to determine the best student. Furthermore, based on this functional evaluation, the population is segregated into four groups. Then the performance of each student belonging to different groups (Group-I, Group-II, Group-III, and Group-IV) are updated using Equations (23)–(27), respectively, as mentioned in Section 4.1. In the SOS optimization technique, the fitness of the initial ecosystem is obtained by evaluating the MOF. Then each organism of the ecosystem is updated by simulating the three symbiotic interactions, namely mutualism, communalism, and parasitism, between the organisms of the current ecosystem as exposed in Equations (30)–(33), respectively. The fitness of the initial population of HHO is also obtained by evaluating the MOF. Then, the initial HH population is modified in three stages of the algorithm: stage-I (exploration), stage-II (balances exploration and exploitation), and stage-III (exploitation). In stage-I, HH updates their placement using Equation (34) to improve exploration. The balance between exploration and exploitation is achieved in stage-II using Equation (35). The exploitation of the HH population is enhanced in stage-III by simulating four different scenarios as discussed in Section 4.3 using Equations (37), (40), (41), and (44), respectively.

5.3. Implementation Steps

The graphical illustration of the optimal planning of the DN considering different planning schemes as implemented using the metaheuristic techniques is envisaged in Figure 2.

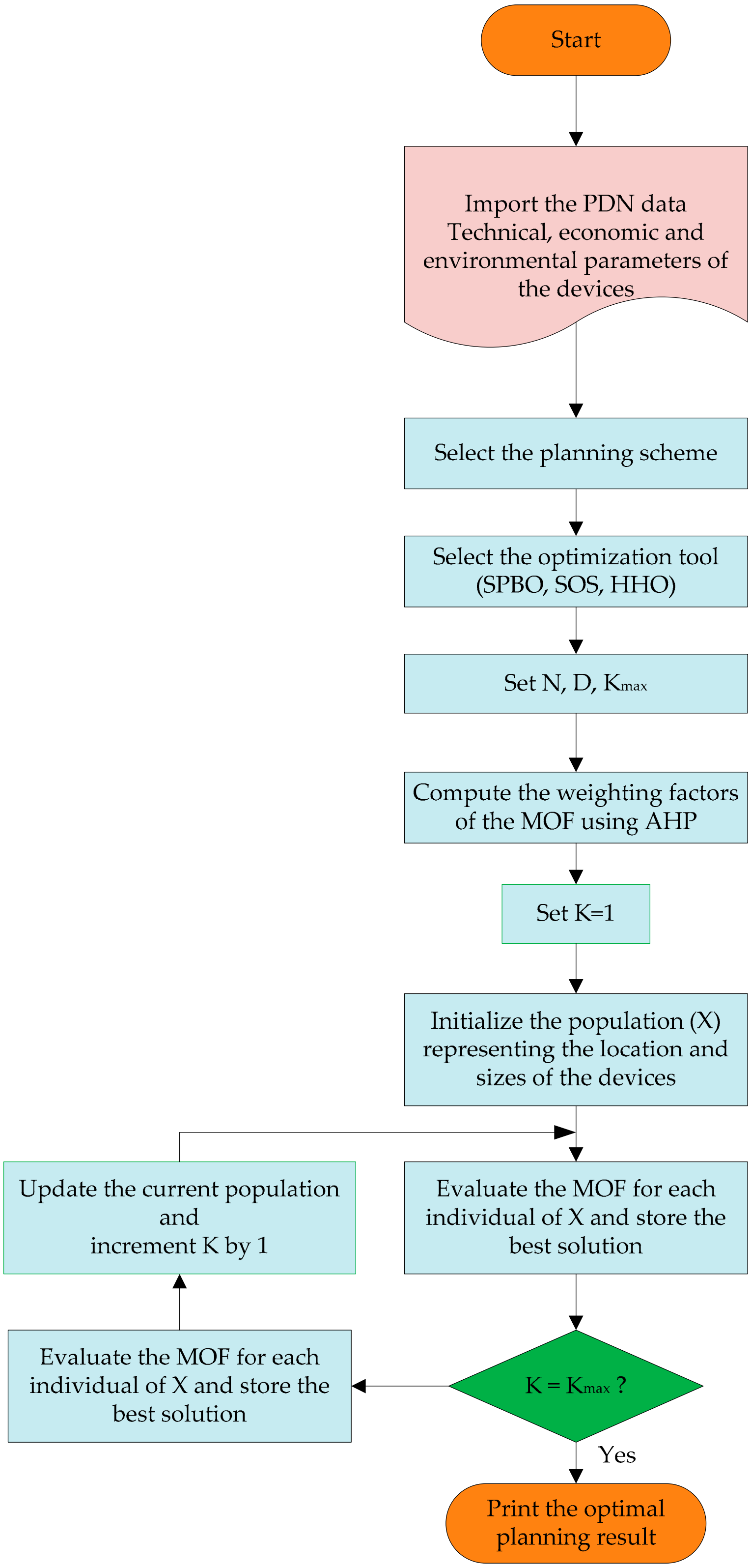

Figure 2. Implementation of optimization tools for the optimal planning of DN.

6. Results and Discussions

The efficacy of the proposed approaches is epitomized by considering two standard test systems, i.e., 33-node and 118-node radial PDN [3]. The MOF, which is the amalgamation of different technical and economic factors for the optimal planning of the PDN, is evaluated using a backward–forward sweep load flow [50]. For each metaheuristic approach, population size and a maximum number of iterations of 50 and 100 are set, respectively. The best results of 30 independent trial runs of the algorithms are reported. The description of the test systems and the sizes of the devices considered are presented in Table 2. All simulations were performed on a laptop (Intel(R) Core (TM) i3-6006U CPU @2.00 GHz, 4GB RAM) using a MATLAB 2016a software package.

Table 2. Description of test systems and devices.

Test System	TPL, kW	TQL, kVAr	kW	kVAR	Test System	TPL, kW	TQL, kVAr
33-node	37,150	2300	210.9824	143.0219	0.9038	2000	2000
118-node	22,710	17,041	12,981	978.7196	0.8688	4000	3000

6.1. Performance Assessment of PFM Algorithms

The suitability of the three parameter-free optimization algorithms, SPBO, SOS, and HHO, for the optimal allocations of single-type devices and different combinations of the devices is assessed by considering the above-mentioned eight cases for each test system.

The best results attained by the SPBO, SOS, and HHO algorithms for exclusive D-STATCOM allocations (case-2) for the two test systems are presented in Tables 3 and 4, respectively.

Table 3. Comparison of results for exclusive D-STATCOM allocation (case-2) for 33-bus test system.

Method	DS Size (MVAR)	DS Bus	Ploss (kW)	Vmin (p.u.)	RPLMI	BVVMI	SVSMI	SACMI	MOF
	0.8167	7							
SPBO	0.9799	30	146.5795	0.9496	0.6947	0.3050	0.5613	0.0014	0.6201
	0.5465	15							
	1.0316	30							
SOS	0.5275	15	146.2087	0.9488	0.6930	0.3073	0.5697	0.0014	0.6203
	0.7850	7							
	1.0737	30							
HHO	0.6580	14	146.9252	0.9490	0.6964	0.3109	0.5680	0.0013	0.6230
	0.4773	7							

Table 4. Comparison of results for exclusive D-STATCOM allocation (case-2) for 118-bus test system.

Method	DS Size (MVAR)	DS Bus	Ploss (kW)	Vmin (p.u.)	RPLMI	BVVMI	SVSMI	SACMI	MOF
	2.7412	110							
SPBO	3.0000	71	936.3917	0.9178	0.7214	0.4673	0.6753	0.0019	0.6825
	3.0000	50							
	2.7598	110							
SOS	2.9322	50	929.6233	0.9155	0.7162	0.4795	0.6914	0.0018	0.6835
	2.8516	71							
	2.8169	110							
HHO	1.9906	50	939.5813	0.9161	0.7238	0.5137	0.6874	0.0016	0.6950
	2.8887	71							

A net optimal reactive power of 2.3431 MVAr, 2.3441 MVAr, and 2.2090 MVAr is injected by the D-STATCOMs in the 33-bus test system, as reported by SPBO, SOS, and HHO, respectively. Similarly, for the 118-bus test system, the net optimal reactive power injected by the D-STATCOMs are 8.7412 MVAr, 8.5436 MVAr, and 7.6962 MVAr, respectively, as obtained by the SPBO, SOS, and HHO. Because of the lowest D-STATCOM capacity reported by HHO, the SACMI is the minimum for both test systems when optimized by HHO. However, owing to the larger capacities of D-STATCOMs as achieved by SPBO and SOS, it leads to better improvement in technical indices than HHO. However, in terms of improvement in the overall performance, the SPBO algorithm obtains the best MOF value of 0.6201 and 0.6825 among the three algorithms for both the test systems, respectively.

The convergence characteristic of the three algorithms for case-2 are compared in Figure 3 for 33-node and 118-node test systems, respectively. As noted from the figures, the SPBO algorithm has a better convergence speed as it settles to the optimal value within 30 iterations for both the test systems.

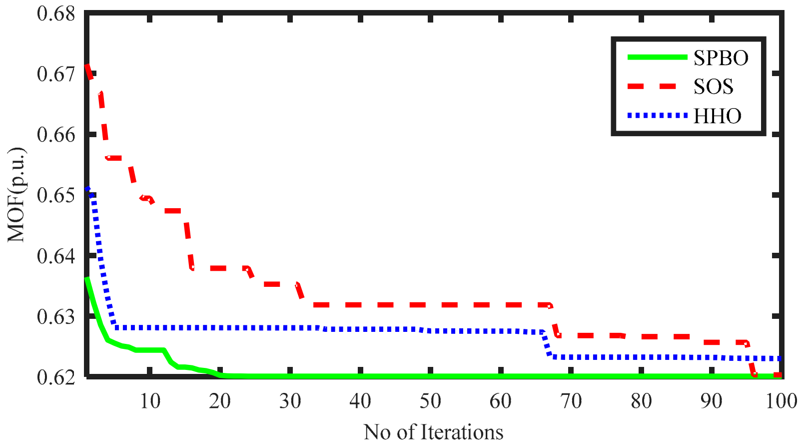

(**a**)

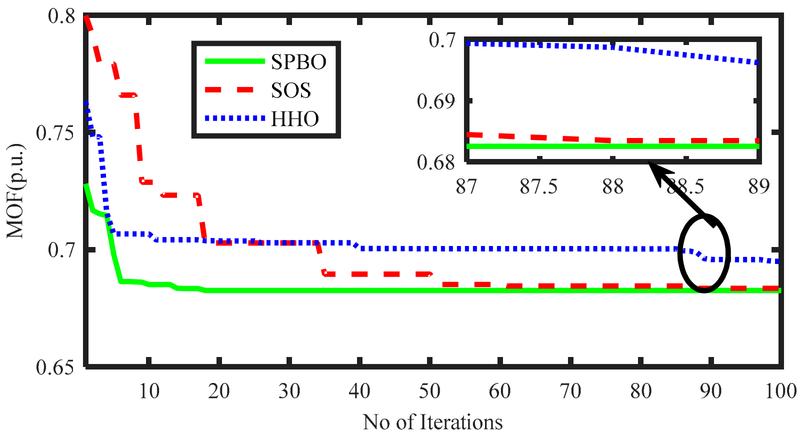

(**b**)

Figure 3. CC of optimization algorithms for case-2. (**a**) 33-bus test system; (**b**) 118-bus test system.

The exclusive allocation of three PV-DGs in 33-node and 118-node PDN are recorded in Tables 5 and 6, respectively. The total real power injection by the three PV-DGs for the 33-node test system is 3.5861 MW, 3.6195 MW, and 3.5665 MW, as achieved by SPBO, SOS, and HHO, respectively. Similarly, for the 118-node test systems, the net real power injection obtained by SPBO, SOS, and HHO is in sequence 10.3908 MW, 10.4210 MW, and 10.5184 MW, respectively. As noted from Tables 5 and 6, SPBO leads the table in terms of the minimum value of MOF compared to the other two algorithms for both test systems. Furthermore, the integration of PV-DGs has improved performance indices (RPLMI, BVVMI, SVSMI, and SACMI) for both test systems compared to that of exclusive DSTATCOM insertion.

Table 5. Comparison of results for exclusive PV-DG allocation (case-3) for 33-bus test system.

Method	DG Size (MW))	DG Bus	Ploss (kW)	Vmin (p.u.)	RPLMI	BVVMI	SVSMI	SACMI	MOF
	1.3114	24							
SPBO	1.3384	30	78.6331	0.9803	0.3727	0.0433	0.2296	0.1369	0.2735
	0.9363	13							
	1.3503	24							
SOS	0.9454	13	78.8536	0.9801	0.3737	0.0425	0.2318	0.1293	0.2737
	1.3238	30							
	1.3778	30							
HHO	1.3129	24	78.6346	0.9807	0.3727	0.0451	0.2249	0.1415	0.2737
	0.8758	14							

Table 6. Comparison of results for exclusive PV-DG allocation (case-3) for 118-bus test system.

Method	DG Size (MW)	DG Bus	Ploss (kW)	Vmin (p.u.)	RPLMI	BVVMI	SVSMI	SACMI	MOF
	3.8704	49							
SPBO	3.4615	71	686.0218	0.9561	0.5285	0.2346	0.3817	0.7130	0.4652
	3.0589	110							
	3.2596	110							
SOS	3.6949	49	685.0649	0.9562	0.5278	0.2349	0.3816	0.7293	0.4660
	3.4665	71							
	3.2988	71							
HHO	3.6066	109	682.2693	0.9556	0.5256	0.2394	0.3861	0.7377	0.4666
	3.6130	50							

Figure 4 depicts the convergence curves of the three algorithms as applied to exclusive PV-DGs allocations to minimize the MOF. From the said figure, it is evident that the convergence speed of the SPBO algorithm is the fastest, followed by HHO and SOS, which proves the efficiency of the SPBO algorithm to solve the optimal PV-DG allocation.

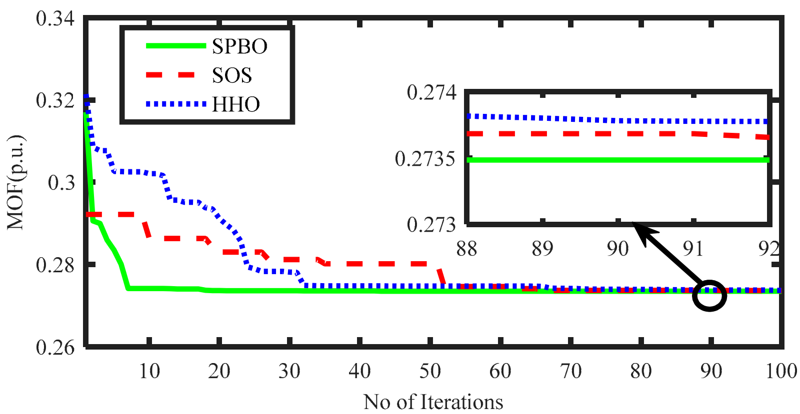

(**a**)

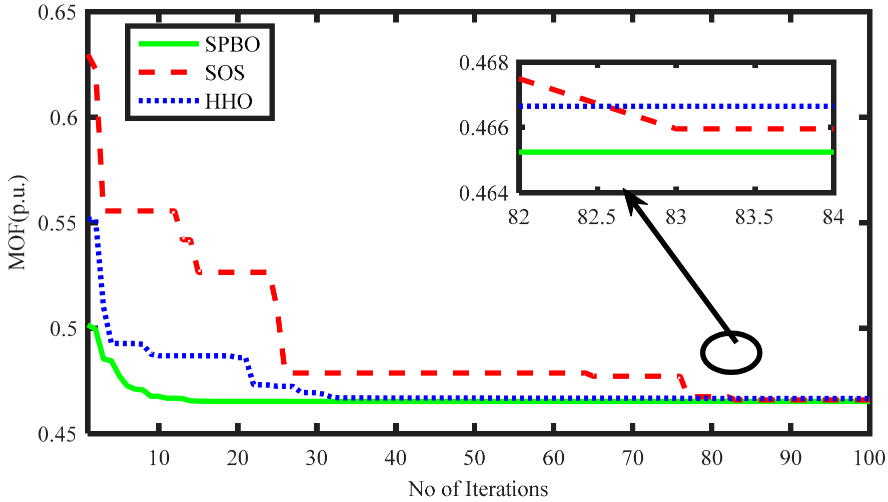

(**b**)

Figure 4. CC of optimization algorithms for case-3. (**a**) 33-bus test system; (**b**) 118-bus test system.

Tables 7 and 8 compare the optimal results for allocating three GT-DGs on the 33-node and 118-node test systems. The net sizes of GT-DG as computed by SPBO, SOS, and HOH are 3.6087 MVA, 3.5487 MVA, and 3.6297 MVA, respectively, for the 33-node test system and 10.8680 MVA, 10.6280 MVA, and 10.5540 MVA, respectively, for the 118-node test system. As GT-DGs operate at a 0.9 power factor, their sizes are marginally larger than the PV-DGs. SPBO achieves minimum MOF value for both the test systems, which proves its supremacy over the other two algorithms considered.

Table 7. Comparison of results for exclusive GT-DG allocation (case-4) for 33-bus test system.

Method	DG Size (MW)	DG Bus	Ploss (kW)	Vmin (p.u.)	RPLMI	BVVMI	SVSMI	SACMI	MOF
SPBO	1.0915 1.3138 0.8425	24 30 13	18.9542	0.9941	0.0898	0.0022	0.0939	0.1973	0.1350
SOS	0.8376 1.0832 1.2730	13 24 30	18.6561	0.9937	0.0884	0.0030	0.1039	0.2097	0.1353
HHO	0.9702 0.9245 1.3720	12 24 30	20.9962	0.9941	0.0995	0.0027	0.0708	0.1934	0.1388

Table 8. Comparison of results for exclusive GT-DG allocation (case-4) for 118-bus test system.

Method	DG Size (MW)	DG Bus	Ploss (kW)	Vmin (p.u.)	RPLMI	BVVMI	SVSMI	SACMI	MOF
SPBO	3.5252 3.2370 3.0190	50 71 110	384.4106	0.9603	0.2961	0.1543	0.3474	0.7300	0.3634
SOS	2.9805 3.3001 3.2846	110 50 71	384.7075	0.9603	0.2964	0.1576	0.3473	0.7492	0.3642
HHO	3.4403 3.4589 2.5994	50 71 110	395.6196	0.9605	0.3048	0.15 79	0.3458	0.7356	0.3680

The convergence characteristic of three considered algorithms for optimal GT-DG allocation to minimize the MOF for 33-node and 118-node test systems are shown in Figure 5, respectively. It can be noted from Figure 5 that the SPBO algorithm achieves the fastest convergence speed as compared to SOS and HHO algorithms for both the test systems. Further, the SPBO algorithm converges to the optimal results within 10 iterations for both the test systems.

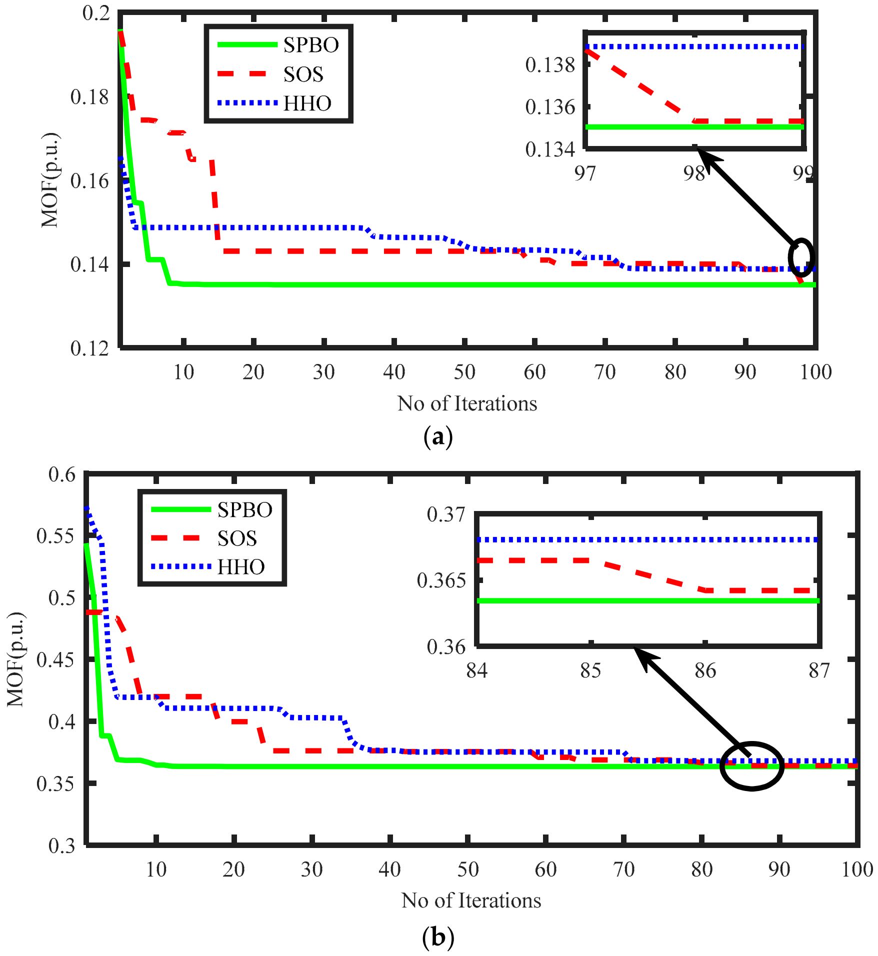

Figure 5. CC of optimization algorithms for case-4. (**a**) 33-bus test system; (**b**) 118-bus test system.

The outcomes of simultaneous allocation of D-STATCOMs and PV-DGs using the studied algorithms are presented in Tables 9 and 10 for both test systems. The optimal effective sizes of the D-STATCOMs and PV-DGs are (1.9081 MVAr, 2.9477 MW), (1.8138 MVAr, 3.3573 MW), and (1.3148 MVAr, 3.1555 MW) for the 33-node test system as obtained by SPBO, SOS, and HHO, respectively. Similarly, for the 118-node test system, the optimal effective sizes of the D-STATCOMs and PV-DGs are in sequence (7.0012 MVAr, 9.9368 MW), (5.6637 MVAr, 9.2612 MW), and (7.0693 MVAr, 10.4279 MW) as obtained by SPBO, SOS, and HHO, respectively. It can be noted that the effective sizes of the individual devices for simultaneous allocation (case-5) are smaller as compared to that of allocation of individual devices (case-2 and case-3). The minimum MOF for both test systems is recorded by the SPBO algorithm, which is 0.0656 p.u. and 0.2825 p.u., respectively.

Table 9. Comparison of results for simultaneous DS and PV-DG allocation (case-5) for 33-bus test system.

Method	DS Size (MVAR)	DS Bus	DG Size (MW)	DG Bus	Ploss (kW)	Vmin (p.u.)	RPLMI	BVVMI	SVSMI	SACMI	MOF
	0.4219	25	1.1474	24							
SPBO	0.4862	12	0.9677	30	12.3286	0.9940	0.0584	0.0030	0.1004	0.2655	0.0656
	1.0000	30	0.8326	13							
	0.6266	8	0.8735	32							
SOS	0.9076	30	0.9020	13	18.8355	0.9936	0.0893	0.0022	0.0905	0.1726	0.0771
	0.2796	25	1.5818	23							
	0.3089	7	1.1902	24							
HHO	0.2515	11	1.0323	30	17.5064	0.9928	0.0830	0.0043	0.0955	0.2195	0.0774
	0.7544	30	0.9330	13							

Table 10. Comparison of results for simultaneous DS and PV-DG allocation (case-5) for 118-bus test system.

Method	DS Size (MVAR)	DS Bus	DG Size (MW)	DG Bus	Ploss (kW)	Vmin (p.u.)	RPLMI	BVVMI	SVSMI	SACMI	MOF
	2.7327	50	4.0000	35							
SPBO	2.3494	110	3.1050	71	356.7143	0.9609	0.2748	0.1406	0.3427	0.6873	0.2825
	1.9191	72	2.8318	110							
	1.6192	75	2.8933	112							
SOS	2.1201	109	3.3768	71	397.2199	0.9602	0.3060	0.1690	0.3482	0.7775	0.3146
	1.9244	51	2.9911	34							
	2.5026	89	3.8947	71							
HHO	2.7468	35	3.2659	35	454.8666	0.9611	0.3504	0.1330	0.3407	0.7609	0.3328
	1.8199	110	3.2673	109							

The convergence characteristic for simultaneous allocation of D-STATCOMs and PV-DGs by the three algorithms for the 33-node and 118-node test systems are shown in Figure 6. The SPBO algorithm converges to the optimal results at about 40 iterations for both test systems, which is the minimum among the three algorithms. The faster convergence speed of the SPBO algorithm is also evident from the said figures.

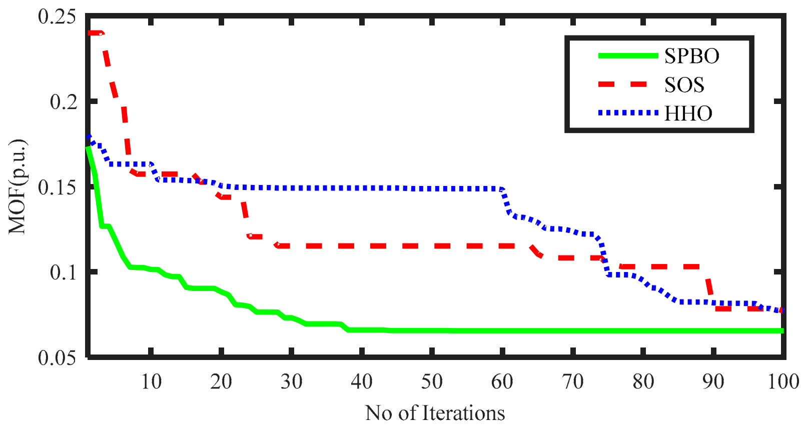

(**a**)

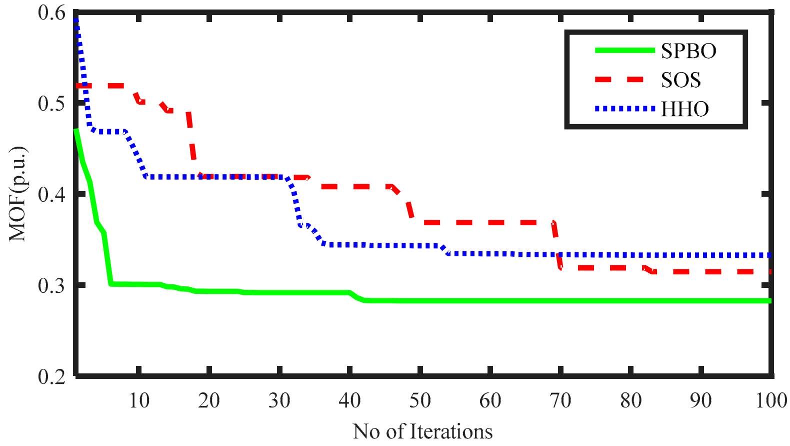

(**b**)

Figure 6. CC of optimization algorithms for case-5. (**a**) 33-bus test system; (**b**) 118-bus test system.

The results of simultaneous allocation of D-STATCOMs and GT-DGs using SPBO, SOS, and HHO algorithms are presented in Tables 11 and 12 for both the test systems. The optimal effective sizes of the D-STATCOMs and GT-DGs are (1.9081 MVAr, 2.9477 MW), (1.8138 MVAr, 3.3573 MW), and (1.3148 MVAr, 3.1555 MW) for the 33-node test system as obtained by SPBO, SOS, and HHO, respectively. Similarly, for the 118-node test system, the optimal effective sizes of the D-STATCOMs and GT-DGs are in sequence (7.0012 MVAr, 9.9368 MW), (5.6637 MVAr, 9.2612 MW), and (7.0693 MVAr, 10.4279 MW) as obtained by SPBO, SOS, and HHO, respectively. It can be noted that the effective sizes of the individual devices for simultaneous allocation (case-5) are smaller as compared to that of allocation of individual devices (case-2 and case-3). The minimum MOF for both the test systems is recorded by the SPBO algorithm, which is 0.1050 p.u. and 0.3057 p.u., respectively.

Table 11. Comparison of results for simultaneous DS and GT-DG allocation (case-6) for 33-bus test system.

Method	DS Size (MVAR)	DS Bus	DG Size (MW)	DG Bus	Ploss (kW)	Vmin (p.u.)	RPLMI	BVVMI	SVSMI	SACMI	MOF
	0.1221	21	1.0814	30							
SPBO	0.4485	7	0.8108	13	11.2484	0.9956	0.0533	0.0012	0.0542	0.9942	0.1050
	0.2837	32	1.0657	24							
	0.1301	31	0.7209	13							
SOS	0.0905	9	1.1221	30	13.0950	0.9934	0.0621	0.0033	0.0843	0.9899	0.1139
	0.6526	6	0.8086	25							
	0.1045	30	0.9969	12							
HHO	0.4822	30	0.9305	30	13.3973	0.9934	0.0635	0.0031	0.0790	0.9935	0.1143
	0.6184	3	0.9628	24							

Table 12. Comparison of results for simultaneous DS and GT-DG allocation (case-6) for 118-bus test system.

Method	DS Size (MVAR)	DS Bus	DG Size (MW)	DG Bus	Ploss (kW)	Vmin (p.u.)	RPLMI	BVVMI	SVSMI	SACMI	MOF
	1.8630	40	3.4937	50							
SPBO	1.9242	80	2.8152	72	317.4696	0.9679	0.2446	0.0902	0.2843	1.5769	0.3057
	1.3316	96	3.0296	110							
SOS	1.1757	99	2.8903	110	328.5501	0.9617	0.2531	0.1027	0.3359	1.5626	0.3180

	1.6938	34	2.8180	72							
	1.6039	83	3.3801	50							
	2.0581	86	2.7324	110							
HHO	2.4914	40	3.3486	50	338.2096	0.9651	0.2605	0.1021	0.3075	1.5996	0.3220
	0.3537	113	3.3498	71							

The convergence characteristic for simultaneous allocation of D-STATCOMs and GT-DGs by the three algorithms for the 33-node and 118-node test systems are shown in Figure 7. The SPBO algorithm shows a faster convergence speed than the SOS and HHO algorithms for both test systems. Furthermore, the SPBO algorithm converges to the optimal results within 30 and 40 iterations for the 33-node test systems and 118-node test systems, respectively, the minimum among the three algorithms.

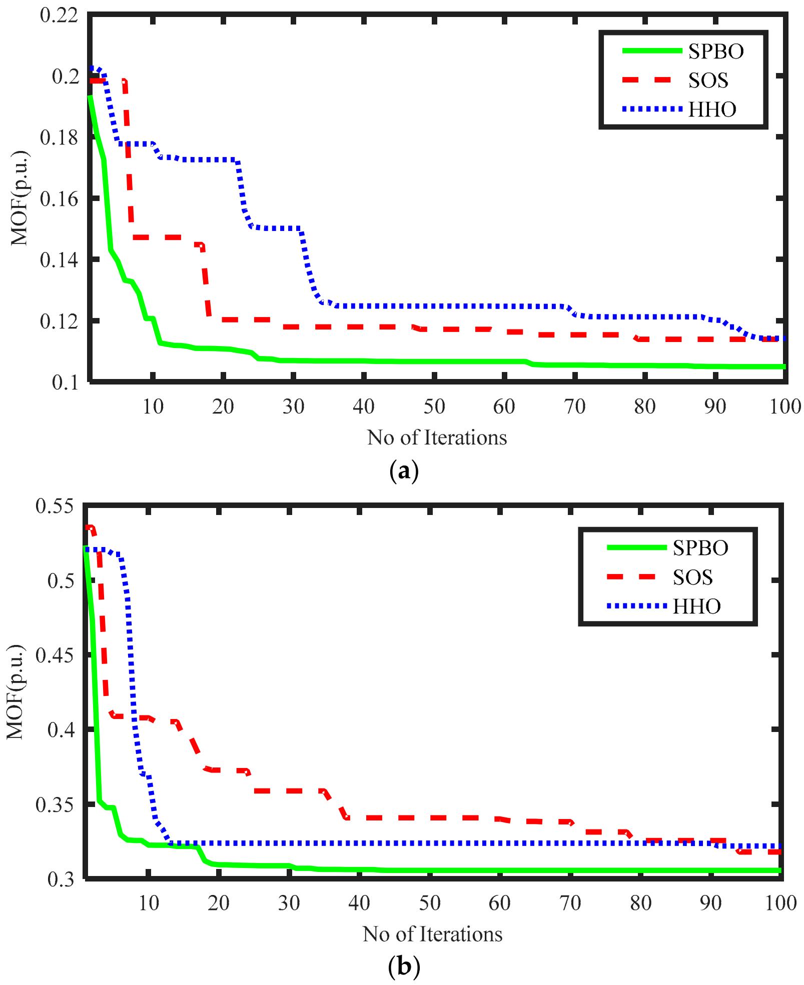

Figure 7. CC of optimization algorithms for case-6. (**a**) 33-bus test system; (**b**) 118-bus test system.

The simultaneous allocation of D-STATCOMs and two PV-DGs and one GT-DGs using the SPBO, SOS, and HHO algorithms are presented in Tables 13 and 14 for both test systems. The optimal effective sizes of the D-STATCOMs and DGs are (1.6375 MVAr, 3.0251 MW), (1.9040 MVAr, 3.7934 MW), and (1.4300 MVAr, 2.8257 MW) for the 33-node test system as obtained by SPBO, SOS, and HHO, respectively. Similarly, for the 118-node test system, the optimal effective sizes of the D-STATCOMs and DGs are in sequence (7.4882 MVAr, 9.7180 MW), (7.0897 MVAr, 8.4920 MW), and (5.3633 MVAr, 8.4624 MW) as obtained by SPBO, SOS, and HHO, respectively. The SPBO algorithm reports the minimum MOF for both test systems, which is 0.0734 p.u. and 0.2827 p.u., respectively.

Table 13. Comparison of results for simultaneous DS and 2 PV-DG and 1 GT-DG allocation (case-7) for 33-bus test system.

Method	DS Size (MVAR)	DS Bus	DG Size (MW)	DG Bus	Ploss (kW)	Vmin (p.u.)	RPLMI	BVVMI	SVSMI	SACMI	MOF
SPBO	0.3886 0.8920 0.3569	7 30 25	1.2583 0.9603 0.8065	24 30 13	11.8232	0.9941	0.0560	0.0022	0.0705	0.4469	0.0734
SOS	0.2659 0.9996 0.6385	21 30 24	1.8492 1.1064 0.8378	3 28 13	21.4769	0.9923	0.1018	0.0029	0.0916	0.2791	0.0925
HHO	0.1932 0.8978 0.3390	25 6 11	0.8445 0.8708 1.1104	13 25 30	15.2584	0.9939	0.0723	0.0024	0.0728	0.5691	0.0922

Table 14. Comparison of results for simultaneous DS and 2 PV-DG and 1 GT-DG allocation (case-7) for 118-bus test system.

Method	DS Size (MVAR)	DS Bus	DG Size (MW)	DG Bus	Ploss (kW)	Vmin (p.u.)	RPLMI	BVVMI	SVSMI	SACMI	MOF
SPBO	2.7782 2.3608 2.3492	50 79 110	4.0000 2.8293 2.8887	35 110 72	333.0302	0.9619	0.2566	0.1130	0.3348	0.9484	0.2827
SOS	2.2048 2.6761 2.2088	83 111 51	3.4071 2.4584 2.6265	35 111 72	372.5530	0.9609	0.2870	0.1323	0.3430	0.9705	0.3079
HHO	2.0932 2.5559 0.9833	55 70 50	2.8687 2.4563 3.1374	50 74 110	400.9431	0.9604	0.3089	0.1650	0.3468	1.0668	0.3353

From the convergence characteristics of case-7 (as displayed in Figure 8), it may be noted that the SPBO algorithm converges to the optimal value within 30 iterations for both test systems, which is the fastest among the three algorithms.

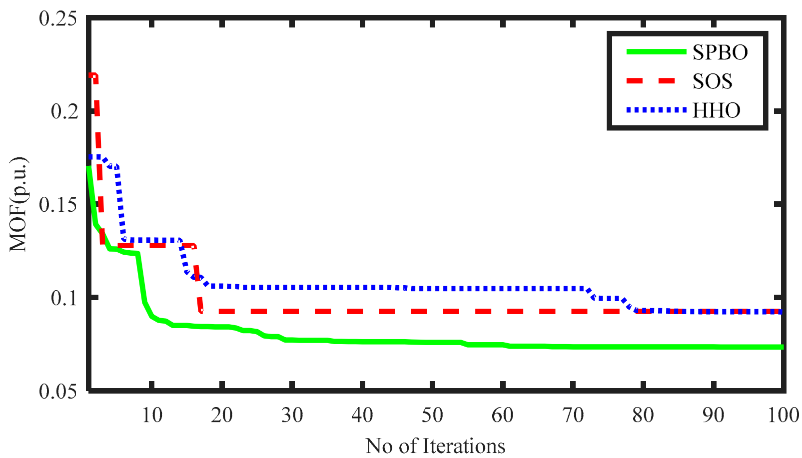

(**a**)

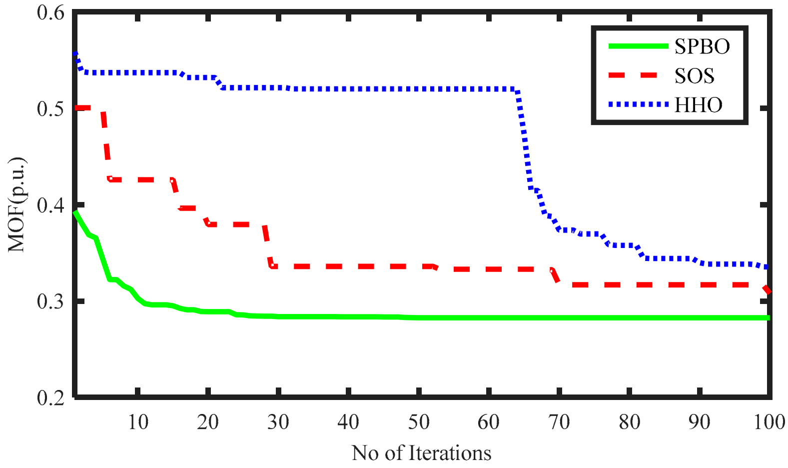

(**b**)

Figure 8. CC of optimization algorithms for case-7. (**a**) 33-bus test system; (**b**) 118-bus test system.

The results of simultaneous allocation of D-STATCOMs and one PV-DG and two GT-DGs using the SPBO, SOS, and HHO algorithms are presented in Tables 15 and 16 for both test systems. The optimal effective sizes of the D-STATCOMs and DGs are (1.1024 MVAr, 3.0533 MW), (1.3173 MVAr, 3.3508 MW), and (0.2186 MVAr, 3.2191 MW) for the 33-node test system as obtained by SPBO, SOS, and HHO, respectively. Similarly, for the 118-node test system, the optimal effective sizes of the D-STATCOMs and DGs are in sequence (7.7064 MVAr, 8.8736 MW), (6.3977 MVAr, 8.8652MW), and (1.7736 MVAr, 9.1159 MW) as obtained by SPBO, SOS, and HHO, respectively. The SPBO algorithm once again reports the minimum MOF for both test systems, which is 0.0892 p.u. and 0.2964 p.u., respectively.

Table 15. Comparison of results for simultaneous DS and 1 PV-DG and 2 GT-DG allocation (case-8) for 33-bus test system.

Method	DS Size (MVAR)	DS Bus	DG Size (MW)	DG Bus	Ploss (kW)	Vmin (p.u.)	RPLMI	BVVMI	SVSMI	SACMI	MOF
SPBO	0.3544	31	1.2310	24	11.4939	0.9941	0.0545	0.0018	0.0705	0.6917	0.0892
	0.3790	25	1.0075	30							
	0.3690	7	0.8148	13							
SOS	0.3586	6	1.7039	23	18.6746	0.9904	0.0885	0.0066	0.1134	0.5821	0.1082
	0.5685	32	0.7775	13							
	0.3902	32	0.8694	30							
HHO	0.1192	32	1.0559	24	19.6031	0.9936	0.0929	0.0033	0.0763	0.7405	0.1174
	0.0235	7	1.1075	30							
	0.0759	31	1.0557	12							

Table 16. Comparison of results for simultaneous DS and 1 PV-DG and 2 GT-DG allocation (case-8) for 118-bus test system.

Method	DS Size (MVAR)	DS Bus	DG Size (MW)	DG Bus	Ploss (kW)	Vmin (p.u.)	RPLMI	BVVMI	SVSMI	SACMI	MOF
SPBO	3.0000 2.3483 2.3581	31 110 79	2.8295 3.1552 2.8889	110 50 72	312.6631	0.9624	0.2409	0.1101	0.3303	1.3042	0.2964
SOS	1.8613 2.2476 2.2888	110 79 38	2.5055 2.6688 3.6909	113 73 50	352.0253	0.9623	0.2712	0.1195	0.3313	1.2840	0.3159
HHO	0.3557 0.4810 0.9369	71 44 74	2.6719 3.1776 3.2664	73 50 110	373.8004	0.9576	0.2880	0.1646	0.3702	1.3422	0.3437

From the convergence characteristics of case-8 (as displayed in Figure 9), it may be noted that the SPBO algorithm converges to the optimal value within 30 iterations for the 33-node and 118-node test systems, which is the fastest among the three algorithms.

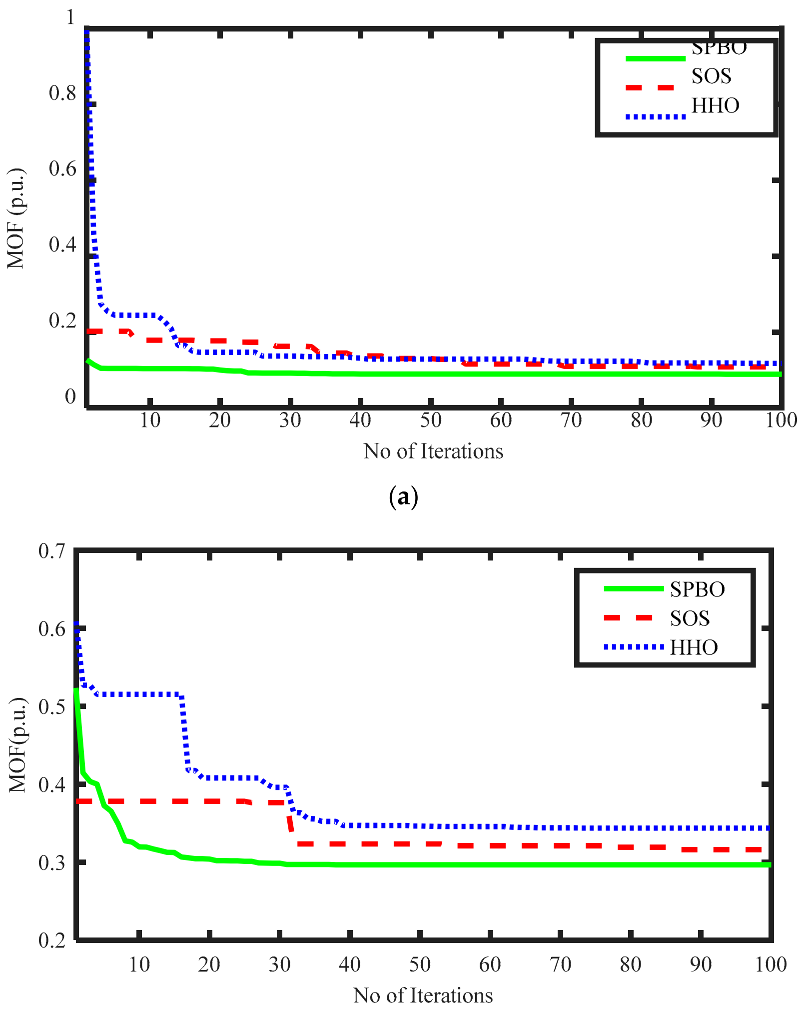

(**a**)

(**b**)

Figure 9. CC of optimization algorithms for case-8. (**a**) 33-bus test system; (**b**) 118-bus test system.

6.2. Statistical Analysis

The supremacy of the SPBO algorithm among the other two parameter-free optimization algorithms, namely SOS and HHO, is further established by conducting a statistical analysis. Tables 17 and 18 report the statistical features such as the minimum MOF, maximum MOF, average MOF, and standard deviation of MOF for the results obtained by the three algorithms for solving optimal planning of the PDN considering all cases except the base case for both test systems. It may be noted that the SPBO algorithm yields the minimum value for all statistical features considered across all cases and for both test systems. The SPBO algorithm is also found to be the most robust algorithm of the lot, as it reports the minimum of the standard deviation value for all the considered cases. The box plots of the results (shown in Figures 10 and 11) obtained by different studied algorithms for optimal PDN planning also reveal the superiority of the SPBO algorithm over other compared algorithms.

Table 17. Statistical performance of different methods for 33-bus system.

Cases	Methods	Minimum MOF	Maximum MOF	Average MOF	SD of MOF
	SPBO	0.6825	0.6825	0.6825	0.0000
2	SOS	0.6835	0.6940	0.6895	0.0028
	HHO	0.6950	0.8223	0.7499	0.0321
	SPBO	0.4652	0.4652	0.4652	0.0000
3	SOS	0.4660	0.4771	0.4698	0.0025
	HHO	0.4666	0.6141	0.5330	0.0546
	SPBO	0.3634	0.3634	0.3634	0.0000
4	SOS	0.3642	0.3780	0.3680	0.0031
	HHO	0.3680	0.5707	0.4489	0.0785
	SPBO	0.2825	0.2902	0.2838	0.0014
5	SOS	0.3146	0.3707	0.3420	0.0151
	HHO	0.3328	0.5394	0.4372	0.0525
	SPBO	0.3057	0.3108	0.3070	0.0014
6	SOS	0.3180	0.3464	0.3314	0.0067
	HHO	0.3220	0.5289	0.4303	0.0607
	SPBO	0.2827	0.2846	0.2832	0.0006
7	SOS	0.3079	0.3420	0.3257	0.0089
	SPBO	0.6825	0.6825	0.6825	0.0000
	SOS	0.6835	0.6940	0.6895	0.0028
8	HHO	0.6950	0.8223	0.7499	0.0321
	SPBO	0.4652	0.4652	0.4652	0.0000

Table 18. Statistical performance of different methods for 118-bus system.

Cases	Methods	Minimum MOF	Maximum MOF	Average MOF	SD of MOF
	SPBO	0.6201	0.6201	0.6201	0.0000
2	SOS	0.6203	0.6277	0.6238	0.0021
	HHO	0.6230	0.6594	0.6332	0.0081
	SPBO	0.2735	0.2737	0.2735	0.0000
3	SOS	0.2737	0.2818	0.2768	0.0025
	HHO	0.2737	0.3062	0.2836	0.0081
	SPBO	0.1350	0.1350	0.1350	0.0000
4	SOS	0.1353	0.1460	0.1376	0.0025
	HHO	0.1388	0.1803	0.1571	0.0137

	SPBO	0.0656	0.0757	0.0703	0.0025
5	SOS	0.0771	0.1074	0.0946	0.0076
	HHO	0.0774	0.2266	0.1353	0.0385
	SPBO	0.1050	0.1111	0.1069	0.0015
6	SOS	0.1139	0.1440	0.1253	0.0073
	HHO	0.1143	0.2376	0.1583	0.0299
	SPBO	0.0734	0.0861	0.0801	0.0033
7	SOS	0.0925	0.1268	0.1039	0.0079
	SPBO	0.0922	0.2156	0.1372	0.0339
	SOS	0.0892	0.0989	0.0940	0.0020
8	HHO	0.1082	0.1316	0.1150	0.0064
	SPBO	0.1174	0.3025	0.1888	0.0475

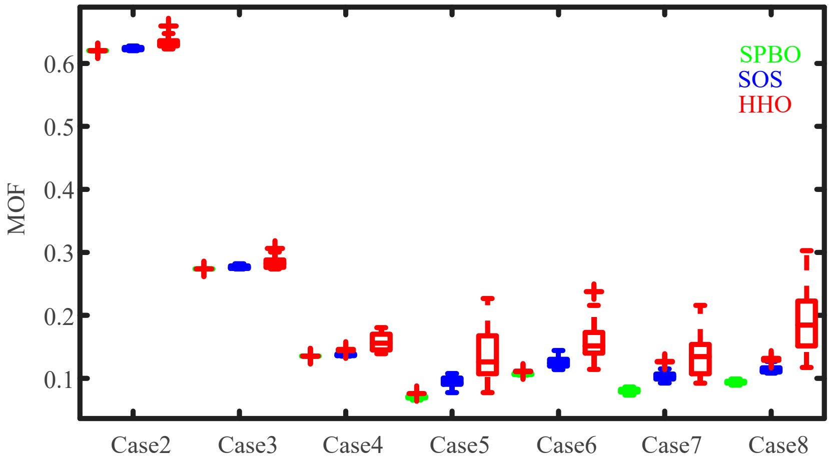

Figure 10. Box plots for 33-node test system.

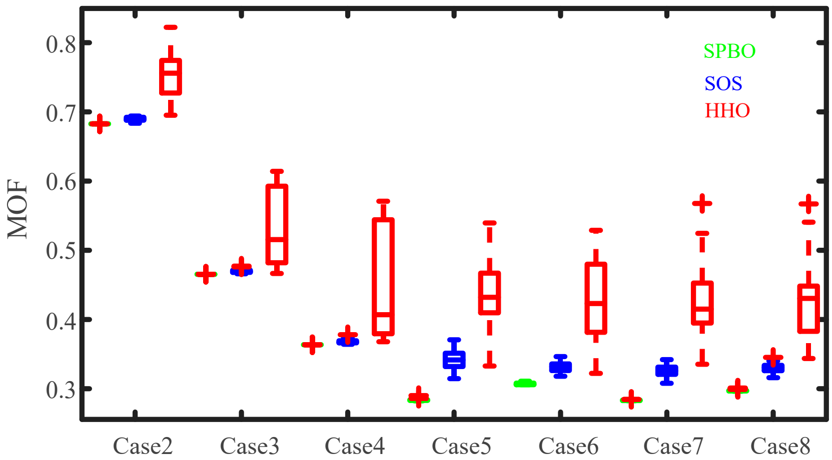

Figure 11. Box plots for 118-node test system.

7. Conclusions

A novel MOF has been developed to assess the performance of three parameter-free metaheuristic algorithms (SPBO, SOS, and HHO) for simultaneous allocation of D-STATCOM and multitype DGs with seven different cases. The MOF included four indices such as RPLMI, BVVMI, SVSMI, and SACMI, accounting for the technological, economic, and environmental benefits of the planning in active distribution networks in the presence of solar PV-DGs, GT-DGs, and D-STATCOMs on two standard test systems (33-bus and 118-bus). The simulation findings clearly indicate that the SPBO method is preferable to the

SOS and HHO algorithms for solving the optimum planning of PDN because it is more resilient, has a faster convergence rate, and is statistically more promising.

Author Contributions: Conceptualization, S.K.D., S.M. and A.Y.A.; methodology, S.K.D. and S.M.; software, S.K.D., S.M. and A.Y.A.; validation, S.K.D., S.M. and A.Y.A.; formal analysis, S.K.D. and A.Y.A.; investigation, S.K.D., S.M. and A.Y.A.; resources, S.K.D. and S.M.; data curation, S.K.D. and S.M.; writing—original draft preparation, S.K.D., S.M. and A.Y.A.; writing—review and editing, S.K.D., S.M., A.Y.A., J.H., Z.W.G.; visualization, S.K.D. and S.M.; supervision, S.K.D., S.M., A.Y.A., Z.W.G.; project administration, S.M., A.Y.A.; funding acquisition, S.M., A.Y.A., J.H., Z.W.G. All authors have read and agreed to the published version of the manuscript.

Funding: This research was supported by the Energy Cloud R&D Program through the National Research Foundation of Korea (NRF) funded by the Ministry of Science, ICT (2019M3F2A1073164).

Institutional Review Board Statement: Not applicable.

Informed Consent Statement: Not applicable.

Data Availability Statement: Not applicable.

Conflicts of Interest: The authors declare no conflict of interest.

References

1. Ganguly, S.; Sahoo, N.C.; Das, D. Recent advances on power distribution system planning: A state-of-the-art survey. *Energy Syst*. **2013**, *4*, 165–193.
2. Shuaibu Hassan, A.; Sun, Y.; Wang, Z. Optimization techniques applied for optimal planning and integration of renewable energy sources based on distributed generation: Recent trends. *Cogent Eng*. **2020**, *7*, 1766394.
3. Mishra, S., Das, D., Paul, S. A comprehensive review on power distribution network reconfiguration. *Energy Syst.* **2017**, *8*, 227–284.
4. Aman, M.M.; Jasmon, G.B.; Bakar, A.H.; Mokhlis, H.; Karimi, M. Optimum shunt capacitor placement in distribution system—A review and comparative study. *Renew. Sustain. Energy Rev*. **2014**, *30*, 429–439.
5. Sambaiah, K.S.; Jayabarathi, T. Loss minimization techniques for optimal operation and planning of distribution systems: A review of different methodologies. *Int. Trans. Electr. Energy Syst*. **2020**, *30*, e12230.
6. Gupta, A.R.; Kumar, A. Deployment of distributed generation with D-FACTS in distribution system: A comprehensive analytical review. *IETE J. Res*. **2019**, 1–8. https://doi.org/10.1080/03772063.2019.1644206.
7. Das, G.; De, M.; Mandal, K.K. Multi-objective optimization of hybrid renewable energy system by using novel autonomic soft computing techniques. *Comput. Electr. Eng*. **2021**, *94*, 107350.
8. Iweh, C.D.; Gyamfi, S.; Tanyi, E.; Effah-Donyina, E. Distributed Generation and Renewable Energy Integration into the Grid: Prerequisites, Push Factors, Practical Options, Issues and Merits. *Energies* **2021**, *14*, 5375.
9. Sanam, J.; Ganguly, S.; Panda, A.K. Distribution STATCOM with optimal phase angle injection model for reactive power compensation of radial distribution networks. *Int. J. Numer. Model. : Electron. Netw. Devices Fields* **2017**, 30, e2240.
10. Montoya, O.D.; Gil-González, W.; Hernández, J.C. Efficient Operative Cost Reduction in Distribution Grids Considering the Optimal Placement and Sizing of D-STATCOMs Using a Discrete-Continuous VSA. *Appl. Sci*. **2021**, *11*, 2175.
11. Dash, S.K.; Mishra, S.; Abdelaziz, A.Y.; Alghaythi, M.L.; Allehyani, A. Optimal Allocation of Distributed Generators in Active Distribution Networks Using a New Oppositional Hybrid Sine Cosine Muted Differential Evolution Algorithm. *Energies* **2022**, *15*, 2267.
12. Nguyen, T.P.; Vo, D.N. Improved stochastic fractal search algorithm with chaos for optimal determination of location, size, and quantity of distributed generators in distribution systems. *Neural Comput. Appl*. **2019**, *31*, 7707–77032.
13. Maheswarapu, S. New hybrid multiverse optimisation approach for optimal accommodation of DGs in power distribution networks. *IET Gener. Transm. Distrib.* **2019**, *13*, 2673–2685.
14. Abo El - Ela, A.A.; Allam, S.M.; Shaheen, A.M.; Nagem, N.A. Optimal allocation of biomass distributed generation in distribution systems using equilibrium algorithm. *Int. Trans. Electr. Energy Syst*. **2021**, *31*, e12727.
15. Truong, K.H.; Nallagownden, P.; Elamvazuthi, I.; Vo, D.N. A quasi-oppositional-chaotic symbiotic organisms search algorithm for optimal allocation of DG in radial distribution networks. *Appl. Soft Comput*. **2020**, *88*, 106067.
16. Hemeida, M.G.; Ibrahim, A.A.; Mohamed, A.A.; Alkhalaf, S.; El-Dine, A.M. Optimal allocation of distributed generators DG based Manta Ray Foraging Optimization algorithm (MRFO). *Ain Shams Eng. J*. **2021**, *12*, 609–619.
17. Hemeida, A.M.; Bakry, O.M.; Mohamed, A.A.; Mahmoud, E.A. Genetic Algorithms and Satin Bowerbird Optimization for optimal allocation of distributed generators in radial system. *Appl. Soft Comput*. **2021**, *111*, 107727.
18. Shaheen, A.M.; Elsayed, A.M.; El-Sehiemy, R.A.; Abdelaziz, A.Y. Equilibrium optimization algorithm for network reconfiguration and distributed generation allocation in power systems. *Appl. Soft Comput*. **2021**, *98*, 106867.
19. Yuvaraj, T.; Ravi, K.; Devabalaji, K.R. DSTATCOM allocation in distribution networks considering load variations using bat algorithm. *Ain Shams Eng. J*. **2017**, *8*, 391–403.

20. Oloulade, A.; Imano, A.M.; Vianou, A.; Tamadaho, H. Optimization of the number, size and placement of D-STATCOM in radial distribution network using Ant Colony Algorithm. *Am. J. Eng. Res. Rev.* **2018**, *1*, 12.
21. Arya, A.K.; Kumar, A.; Chanana, S. Analysis of distribution system with D-STATCOM by gravitational search algorithm (GSA). *J. Inst. Eng. (India): Ser. B*. **2019**, *100*, 207–215.
22. Balamurugan, P.; Yuvaraj, T.; Muthukannan, P. Optimal allocation of DSTATCOM in distribution network using whale optimization algorithm. *Eng. Technol. Appl. Sci. Res*. **2018**, *8*, 3445–3449.
23. Kalia Perumal Rukmani, D.; Thangaraj, Y.; Subramaniam, U.; Ramachandran, S.; Madurai Elavarasan, R.; Das, N.; Baringo, L.; Imran Abdul Rasheed, M. A new approach to optimal location and sizing of DSTATCOM in radial distribution networks using bio-inspired cuckoo search algorithm. *Energies* **2020**, *13*, 4615.
24. Sanam, J. Optimization of planning cost of radial distribution networks at different loads with the optimal placement of distribution STATCOM using differential evolution algorithm. *Soft Comput*. **2020**, *24*, 13269–13284.
25. Dash, S.K.; Mishra, S. Simultaneous Optimal Placement and Sizing of D-STATCOMs Using a Modified Sine Cosine Algorithm. In *Advances in Intelligent Computing and Communication*; Springer: Singapore, 2021; pp. 423–436.
26. Castiblanco-Pérez, C.M.; Toro-Rodríguez, D.E.; Montoya, O.D.; Giral-Ramírez, D.A. Optimal Placement and sizing of D-STATCOM in radial and meshed distribution networks using a discrete-continuous version of the genetic algorithm. *Electronics* **2021**, *10*, 1452.
27. Khan, B.; Redae, K.; Gidey, E.; Mahela, O.P.; Taha, I.B.; Hussien, M.G. Optimal integration of DSTATCOM using improved bacterial search algorithm for distribution network optimization. *Alex. Eng. J*. **2022**, *61*, 5539–5555.
28. Thangaraj, Y.; Kuppan, R. Multi-objective simultaneous placement of DG and DSTATCOM using novel lightning search algorithm. *J. Appl. Res. Technol.* **2017**, *15*, 477–491.
29. Yuvaraj, T.; Ravi, K. Multi-objective simultaneous DG and DSTATCOM allocation in radial distribution networks using cuckoo searching algorithm. *Alex. Eng. J.* **2018**, *57*, 2729–2742.
30. Ganesh, S.; Kanimozhi, R. Meta-heuristic technique for network reconfiguration in distribution system with photovoltaic and D-STATCOM. *IET Gener. Transm. Distrib*. **2018**, *12*, 4524–4535.
31. Yuvaraj, T.;Devabalaji, K.R.; Thanikanti, S.B. Simultaneous allocation of DG and DSTATCOM using whale optimization algorithm. *Iranian J. Sci. Technol. Trans. Electr. Eng*. **2020**, *44*, 879–896.
32. Zellagui, M.; Lasmari, A.; Settoul, S.; El‐Sehiemy, R.A.; El‐Bayeh, C.Z.; Chenni, R. Simultaneous allocation of photovoltaic DG and DSTATCOM for techno-economic and environmental benefits in electrical distribution systems at different loading conditions using novel hybrid optimization algorithms. *Int. Trans. Electr. Energy Syst.* **2021**, *31*, e12992.
33. Chinnaraj, S.G.R.; Kuppan, R. Optimal sizing and placement of multiple renewable distribution generation and DSTATCOM in radial distribution systems using hybrid lightning search algorithm-simplex method optimization algorithm *Comput. Intell.* **2021**, *37*, 1673–1690.
34. Oda, E.S.; Abd El Hamed, A.M.; Ali, A.; Elbaset, A.A.; Abd El Sattar, M.; Ebeed, M. Stochastic optimal planning of distribution system considering integrated photovoltaic-based DG and DSTATCOM under uncertainties of loads and solar irradiance. *IEEE Access* **2021**, *9*, 26541–26555.
35. Eid, A.; Kamel, S.; Zawbaa, H.M.; Dardeer, M. Improvement of active distribution systems with high penetration capacities of shunt reactive compensators and distributed generators using Bald Eagle Search. *Ain Shams Eng. J*. **2022**, *13*, 101792.
36. Ghatak, S.R.; Sannigrahi, S.; Acharjee, P. Optimised planning of distribution network with photovoltaic system, battery storage, and DSTATCOM. *IET Renew. Power Gener.* **2018**, *12*, 1823–1832.
37. Tolabi, H.B.; Ali, M.H.; Rizwan, M. Simultaneous reconfiguration, optimal placement of DSTATCOM, and photovoltaic array in a distribution system based on fuzzy-ACO approach *IEEE Trans. Sustain. Energy* **2015**, *6*, 210–218.
38. Das, B.; Mukherjee, V.; Das, D. Student psychology-based optimization algorithm: A new population based optimization algorithm for solving optimization problems. *Adv. Eng. Softw.* **2020**, *146*, 102804.
39. Kennedy, J.; Eberhart, R. Particle swarm optimization. In Proceedings of the ICNN’95—International Conference on Neural Networks, Perth, WA, Australia, 27 November–1 December 1995; Volume 4; pp. 1942–1948.
40. Rao, R.V.; Savsani, V.J.; Vakharia, D.P. Teaching–learning-based optimization: A novel method for constrained mechanical design optimization problems. *Comput.-Aided Design* **2011**, *43*, 303–315.
41. Yang, X.S.; Deb, S. Engineering optimisation by cuckoo search. *Int. J. Math. Model. Numer. Optimisation* **2010**, *1*, 330–343.
42. Cheng, M.Y.; Prayogo, D. Symbiotic organisms search: A new metaheuristic optimization algorithm. *Comput. Struct.* **2014**, *139*, 98–112.
43. Tanabe, R.; Fukunaga, A. Success-history based parameter adaptation for differential evolution. In Proceedings of the 2013 IEEE Congress on Evolutionary Computation, Cancun, Mexico, 20–23 June 2013; pp. 71–78.
44. Mirjalili, S.; Mirjalili, S.M.; Lewis, A. Grey wolf optimizer. *Adv. Eng. Softw*. **2014**, *69*, 46–61.
45. Dash, S.K.; Mishra, S. Optimal Allocation of Photo-Voltaic Units in Radial Distribution Networks Using a New Student Psychology Based Optimization Algorithm. *Int. J. Electr. Eng. Inf*. **2021**, *13*, 318–335.
46. Balu, K.; Mukherjee, V. Optimal siting and sizing of distributed generation in radial distribution system using a novel student psychology-based optimization algorithm. *Neural Comput. Appl*. **2021**, *33*, 15639–15667.
47. Gharehchopogh, F.S.; Shayanfar, H.; Gholizadeh, H. A comprehensive survey on symbiotic organisms search algorithms. *Artif. Intell. Rev.* **2020**, *53*, 2265–2312.

48. Heidari, A.A.; Mirjalili, S.; Faris, H.; Aljarah, I.; Mafarja, M.; Chen, H. Harris hawks optimization: *Algorithm Appl. Future Gener. Comput. Syst.* **2019**, *97*, 849–872.
49. Wolpert, D.H.; Macready, W.G. No free lunch theorems for optimization. *IEEE Trans. Evol. Comput.* **1997**, *1*, 67–82.
50. Mishra, S. A simple algorithm for unbalanced radial distribution system load flow. In Proceedings of the TENCON 2008-2008 IEEE Region 10 Conference, Hyderabad, India, 19–21 November 2019; pp. 1–6.